Role of AKAP12 in recovery from intestinal inflammation

대장 염증 회복과정에서 AKAP12 단백질의 기능 연구

지도교수 김 규 원

이 논문을 약학박사학위논문으로 제출함
2016년 11월

서울대학교 대학원
약학과 의약생명과학 전공
양 준 모

양 준 모 의 박사학위논문을 인준함
2016년 12월

위 원 장 서 영준 (인)

부위원장 이 호영 (인)

위 원 이 수 재 (인)

위 원 이 정 원 (인)

위 원 김 규 원 (인)

약학박사학위논문

Role of AKAP12 in recovery from intestinal inflammation

대장 염증 회복과정에서 AKAP12 단백질의 기능 연구

2017 년 2 월

서울대학교 대학원

약학과 의약생명과학 전공

양 준 모

ABSTRACT

Role of AKAP12 in recovery from intestinal inflammation

Jun-Mo Yang

Division of Pharmaceutical Bioscience

College of Pharmacy

The Graduate School

Seoul National University

Macrophages exhibit phenotypic plasticity, as they have the ability to switch their functional phenotypes during inflammation and recovery. Simultaneously, the mechanical environment is actively changing. However, how these dynamic alteration affects the macrophage phenotype is unknown. Here, I show that the extracellular matrix (ECM) constructed by AKAP12+ colon mesenchymal cells (CMCs) generates M2 macrophages by regulating their shape during recovery. Notably, round macrophages were present in the linear and

loose ECM of inflamed colons and polarized to the M1 phenotype. In contrast, ramified macrophages emerged in the contracted ECM of recovering colons and mainly expressed M2 macrophage markers. These contracted structures were not observed in the inflamed colons of AKAP12 knockout (KO) mice. Consequently, the proportion of M2 macrophages in inflamed colons was lower in AKAP12 KO mice than in WT mice. In addition, clinical symptoms and histological damage were more severe in AKAP12 KO mice than in WT mice. In experimentally remodelled collagen gels, WT CMCs drove the formation of a more compacted structure than AKAP12 KO CMCs, which promoted the polarization of macrophages toward an M2 phenotype. These results demonstrate that tissue contraction during recovery provides macrophages with the physical cues that drive M2 polarization.

keywords: **Intestinal inflammaton and recovery/ AKAP12/ tissue contraction/ contracted structure/ macrophage shape/ M2 macropahge polarization,**

Student Number: **2011 - 21736**

TABLE OF CONTENTS

LIST OF FIGURES

LIST OF ABBREVIATIONS

AKAP12: A-kinase anchoring protein

α-SMA: alpha-smooth muscle actin

BMDMs: bone-marrow derived macrophages

CD: crohn's disease

CMCs: colon mesenchymal cells

CNS: central nervous system

DEGs: differentially expressed genes

DSS: dextran sulfate sodium

ECM: extracellular matrix

FAK: focal adhesion kinase

IL-10: interleukin- 10

IBD: inflammatroy bowel disease

iNOS: inducible nitic oxide synthases

KO: knock out

LPS: lipopolysaccharide

MMP: Matrix metalloproteinase

RA: retinoic acid

Raldh2: retinaldehyde dehydrogenase2

TGF- β: transforming growth factor- β

TNF-α: tumor necrosis factor

UC: ulcerative colitis

WT: wild type

2D: two-dimensional

3D: three-dimesional

INTRODUCTION

1. Role and plasticity of macrophage

Macrophages are diverse and multifunctional innate immune cells that play a role in many biological processes (Wynn et al., 2013). In performing their various roles, macrophages can adopt many functional phenotypes. Although the phenotype of macrophage appears as spectrum (Mosser and Edwards, 2008), they are generally categorized by activation state as either classically activated (M1, pro-inflammatory) or alternatively activated (M2, anti-inflammatory, tissue healing) (Figure 1) (Sica and Mantovani, 2012). M1 macrophages are characterized by high production of pro-inflammatory cytokines and reactive nitrogen and oxygen intermediates, and, display strong microbicidal and tumoricidal activity. In contrast, M2 macrophages induce tissue remodeling and tumor progression. They also have an immunoregulatory function and efficient phagocytic activity (Sica and Mantovani, 2012). M1-M2 macrophages can switch their phenotypes to other phenotypes. This plasticity of macrophages is attributable to their

ability to change their functional phenotype in response to the prevailing microenvironment. Indeed, in many diseases or biological process, phenotypic presentations of macrophages are actively changing along with altered microenvironment. Due to this dynamics, how the phenotype of macrophage during the process is regulated largely undetermined.

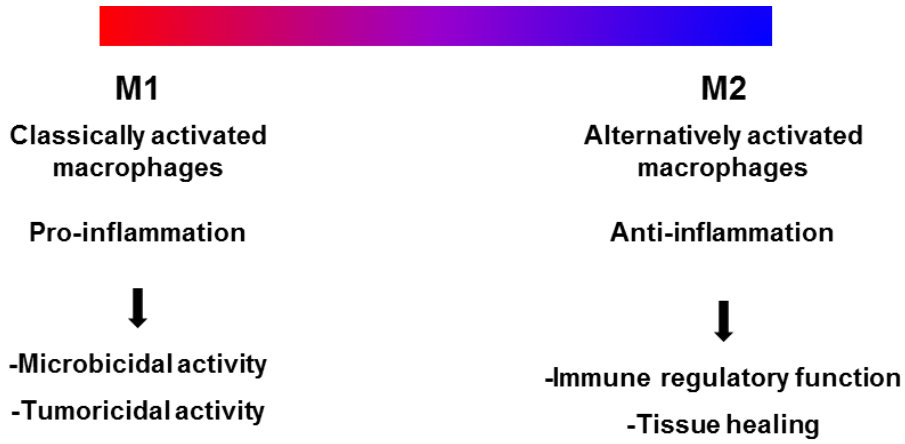

Figure 1. Macrophage activation state and function. A dichromatic spectrum of the two macrophage designations, M1 and M2. The two populations of macrophages including classically activated macrophages, and alternatively activated macrophages.

2. Regulation of macrophage polarization

Much of our current understanding regarding macrophage polarization is limited to how soluble factors affect a macrophage function. For instance, tumor necrosis factor- α (TNF-α), interferon- γ (IFN-γ) and lipopolysaccharide (LPS) drive macrophages to an M1 phenotype, whereas interleukin- 4 (IL-4), interleukin- 10 (IL-10) and transforming growth factor- β (TGF- β) are cytokines that stimulate M2 polarization (Murray et al., 2014).

However, microenvironment is highly complex and involves many factors that can influence manifestation of macrophage phenotype (Figure 2). Because of this imperfect understanding regarding macrophage polarization, selectively targeting macrophages with disease phenotypes has to date proved unsuccessful (Jetten et al., 2014). Therefore, to establish targeting of macrophage polarization as a promising therapeutic strategy, it is necessary to consider other factors that modulate the functional phenotype of macrophage. Recent studies clearly demonstrate that mechanical factors in the microenvironment such as matrix architecture, substrate stiffness, substrate topography, cell shape and intracellular mechanics can regulate the macrophage

phenotype and the function under in vitro conditions (Figure 3) (McWhorter et al., 2015). Furthermore, physical cues can also function synergistically with soluble factors to control macrophage polarization.

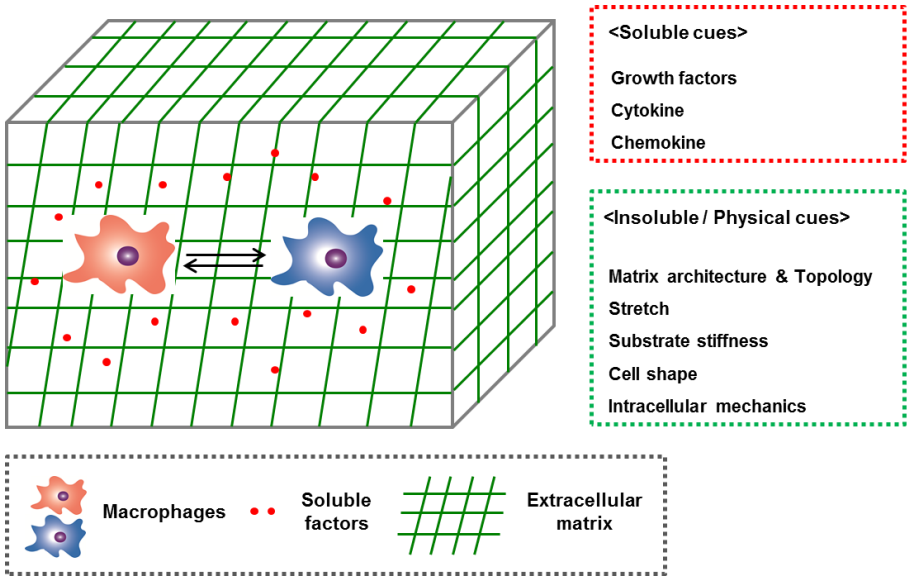

Figure 2. Regulation of macrophage polarization.

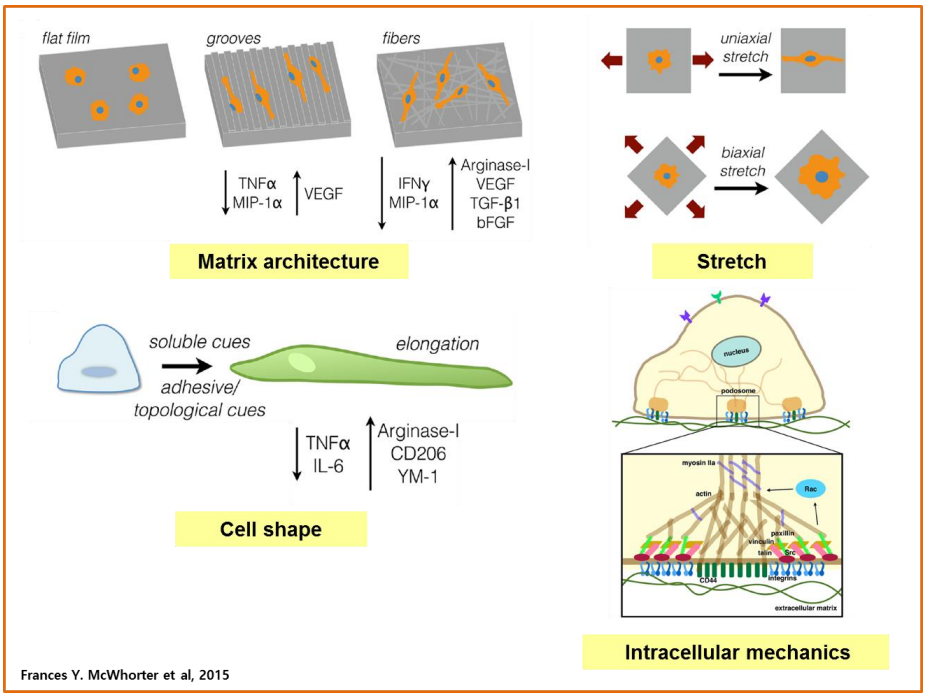

Figure 3. Contribution of mechanical cues on macrophage polarization.

3. Extracellular matrix and macrophage polarization

Many diseases and biological processes are accompanied by dynamic changes in the mechanical microenvironment and the macrophage phenotypes. Inflammation and the recovery process are also accompanied by a dynamic alteration in the functional phenotype of macrophages and the mechanical environment. During inflammation, activated macrophages derived from circulating monocytes or resident tissue macrophages migrate to damaged tissue and become polarized to an M1 phenotype. Subsequently, after the occurrence of inflammation, recovery of the tissue commences and the functional phenotype of macrophage gradually shift to an M2 phenotype (Cao et al., 2015). Simultaneously, the mechanical environment is actively changing. The ECM in the vicinity of the damaged tissue is degraded by several proteolytic enzymes and becomes semi-liquid during the inflammation phase. During the recovery phase, this soft ECM become stiff and tight by regeneration and contraction of the tissue (Rydell-Tormanen et al., 2012). Although these two dynamic changes interacts with each other, the only well-

established one way communications are the promotion of ECM destruction by M1 macrophages and the contribution of M2 macrophages to tissue remodelling by deposition of collagen (Figure 4) (Murray and Wynn, 2011). Nevertheless, how alteration of the mechanical environment affects macrophage polarization during inflammation and recovery is still largely undetermined.

It was recently shown that the ECM structure affects the migratory function of macrophages (Van Goethem et al., 2010). Furthermore, during atherosclerosis, M2 populations dominate within the collagen-rich fibrous cap and adventitia surrounding the plaque and exhibit an elongated morphology (Chinetti-Gbaguidi et al., 2011; Stoger et al., 2012). Despite the evidence suggesting that ECM properties are related to the macrophage function and phenotype, the mechanism whereby the ECM regulates the functional phenotype of macrophage during specific biological processes has not been explored.

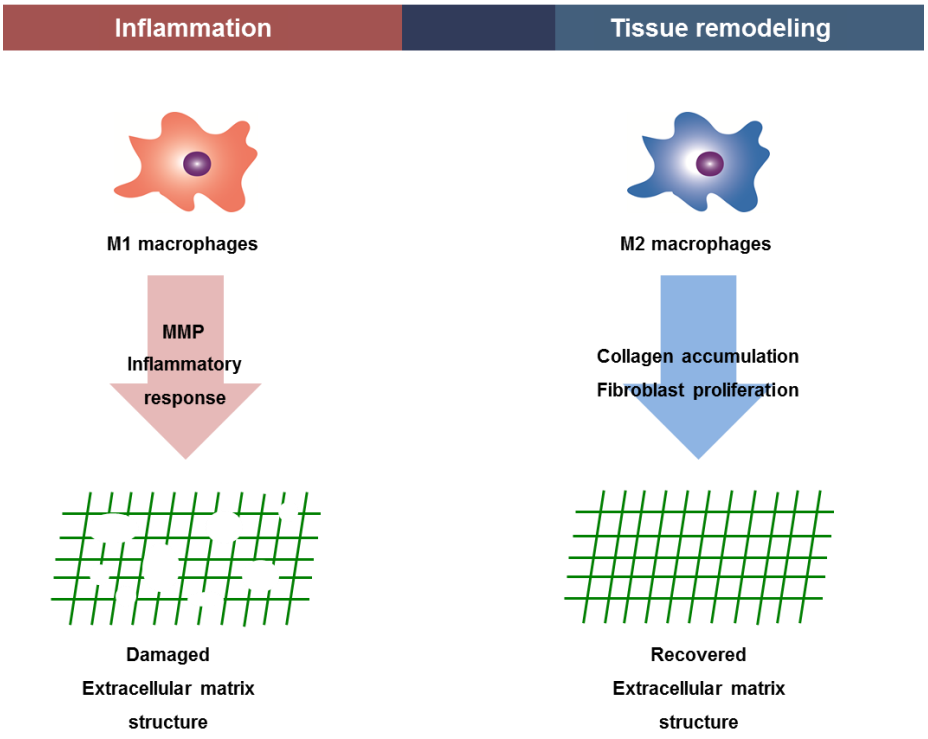

Figure 4. Alteration of macrophage phenotype leads to change of mechanical environment.

4. Myofibroblast and tissue contraction

Myofibroblasts were first observed in healing skin wounds, where it was hypothesized that they were responsible for wound contraction (Gabbiani et al., 1971). These cells are key players for maintaining tissue homeostasis and for orchestrating tissue repair. Myofibroblasts are differentiated from fibroblasts and expresses α-smooth muscle actin. Since focal adhesion, which is a cellular structure that links the extracellular matrix on the outside of the cell, develops to supermature focal adhesion in the myofibroblasts, these cells generate stronger forces than the fibroblast (Figure 5) (Tomasek et al., 2002).

In recovery process after inflammation, ECM, which is degraded by proteolytic enzyme during inflammatory phase, regenerates and remodeled. During this step, cells need strong forces to contract the tissue due to dense microenvironment formed by accumulation of ECM and increased cell population. At that time, a population of myofibroblasts induced by increased TGF-β and mechanical tension increases and promotes tissue contraction. Through tissue contraction, loose matrix restores their original elasticity and turn into a tight and compact matrix structure.

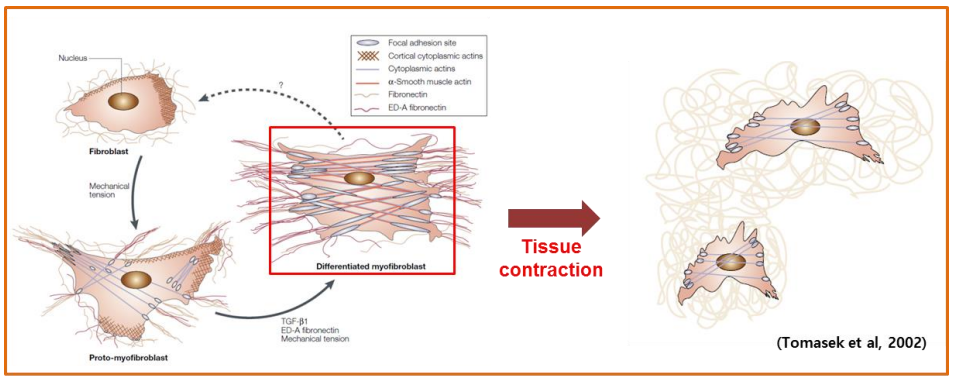

- Myofibroblasts with mature focal adhesion appear in tissue healing phase
- Myfibroblasts exert large mechanical force through mature focal adhesion
- Regenerated tissue is contracted by myofibroblasts

Figure 5. Differentiation of fibrolast to myofibroblast and tissue contraction.

5. AKAP12

A-kinase anchoring protein 12 (AKAP12), a scaffolding protein, has various functions in many biological events (Gelman, 2010). AKAP12 regulates migratory process and cell cycle, vessel integrity, and blood neural barrier differentiation during development (Akakura and Gelman, 2012; Choi et al., 2007; Kwon et al., 2012). As a tumor suppressor protein, suppression of AKAP12 induces prostatic hyperplasia *in vivo* and increases cell invasiveness *in vitro* (Akakura et al., 2008). In addition, our group has recently reported that AKAP12 expressing cells form a physical barrier that surrounds lesions after CNS injury (Figure 6) (Cha et al., 2014a; Cha et al., 2014b).

It was also reported that AKAP12 is expressed in focal adhesion and, under AKAP12 deficient condition, integrin β1 is not clustered and mature focal adhesion is not observed (Su et al., 2013). Thus, AKAP12 is involved in mechanical processes and might have a role in ECM by modulating the cell mechanics. In addition, because AKAP12 functions as promoting formation of stable and mature focal adhesion, it could be included in tissue contraction (Figure 7).

Actually, during brain injury, AKAP12 shows higher expression in

the recovery phase than in the acute inflammation phase. Moreover, the lesion area of AKAP12 KO mice was less contracted than that of WT mice during the recovery phase following CNS injury (Figure 7).

Collectively, I postulate that AKAP12 functions as a regulator of tissue remodelling and contraction, and that the mechanical environment regulated by AKAP12 could modulate disease progression by providing macrophages to mechanical cues during recovery (Figure 8).

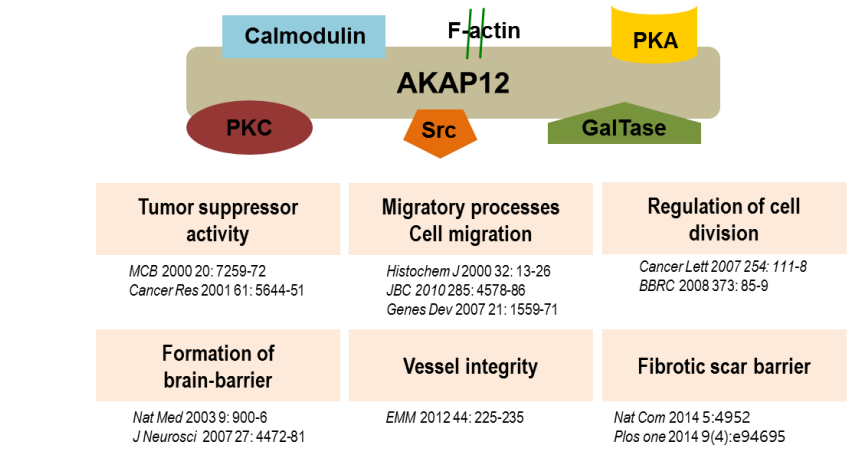

- **Multi-functional scaffolding protein**

  Dynamic reversible platform for multiple signaling such as PKA, PKC, β adrenergic receptor pathway

- **Control of cell migration and cell cycle**

  Regulates the focal adhesion and Integrates cytoskeletal dynamics with cellular signaling cascades

- **Control of cell-cell adhesion**

  Regulates the expression of adhesion proteins and actin arrangement

Figure 6. Various functions of AKAP12.

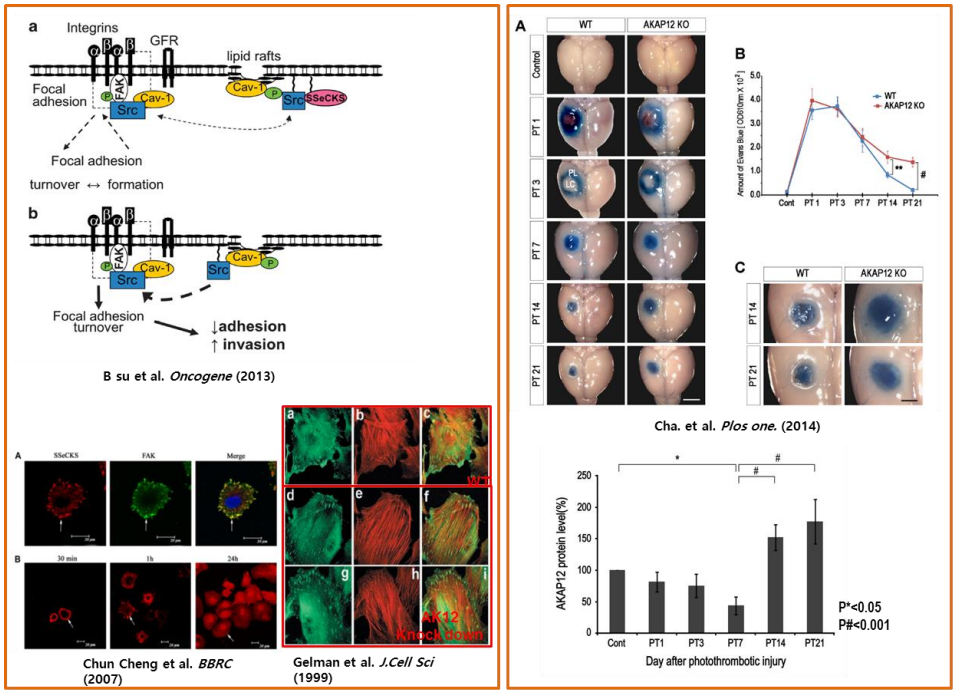

Role of AKAP12 on mechanical properties of cells

Contribution of AKAP12 to tissue healing and contraction

Figure 7. Role of AKAP12 on mechanical properties of the cell and contribution of AKAP12 to tissue healing and contraction.

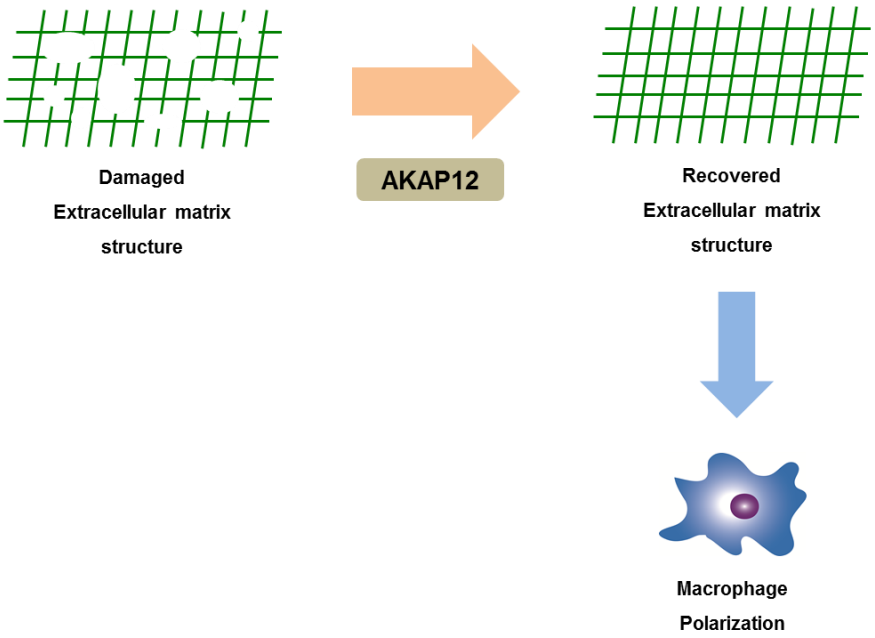

Figure 8. Hypothesis of the study

6. Dextran sulfate sodium-induced colitis

Inflammatory bowel disease (IBD) is a complex multifactorial disease including ulcerative colitis (UC) and Crohn's disease (CD). These two chronic diseases involve inflammation of the intestine. Dextran sulfate sodium (DSS) induced colitis is a murine model that chemically induces the intestinal inflammation (Perse and Cerar, 2012). DSS is a water-soluble, negatively charged sulfated polysaccharide with a highly variable molecular weight ranging from 5 to 1400 kDa.

The DSS-induced colitis model has some advantages when compared to other murine models of intestinal inflammation. For instance, an acute, chronic, or relapsing model can be designed and modified easily by changing the concentration and duration of administration of DSS. Futhermore, chronic phase of DSS-induced colitis resembles the clinical course of human UC (Figure 9).

It is widely accepted that numerous inflammatory mediators such as TNF-α, IL-1 β, IFNγ, IL-10, and IL-12 have been implicated in DSS-induced colitis. In addition, an innate immune system contributes to development of intestinal inflammation (Kuhl et al., 2015). Moreover, macrophages are one of the most abundant innate immune

cells in the colon and closely involved in intestinal inflammation (Heinsbroek SE et al, 2009). Hence, to ameliorate the inflammatory response during intestinal inflammation, it is important to construct non-inflammatory microenvironment that drives the macrophage to a non-inflammatory phenotype.

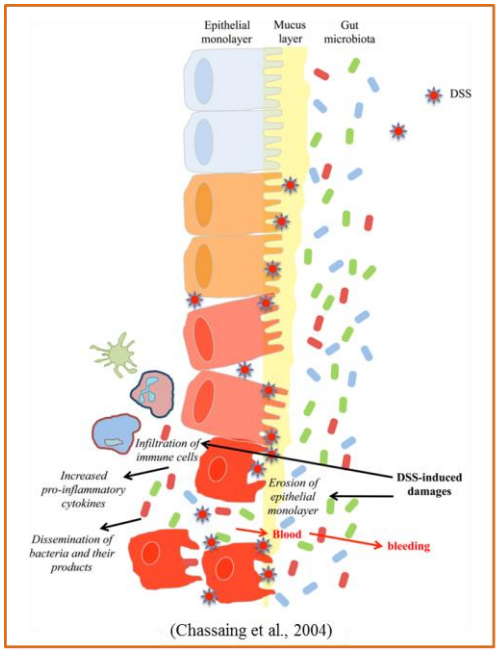

- **Chemically induced intestinal inflammation**

  DSS is a water-soluble, negatively charged sulfated polysaccharide with a highly variable molecular weight ranging from 5 to 1400 kDa.

- **Inflammatory response & innate immune system**

  Innate system including macrophages mainly contribute to development and recovery of intestinal inflammation.

- **Inflammatory bowel diseases (IBD)**

  DSS-induced colitis resembles the clinical course of human UC.

Figure 9. Schematic representation of DSS-induced colitis. (Chassaing et al., 2014)

PURPOSE OF THIS STUDY

Macrophages exhibit phenotypic plasticity, as they have the ability to switch their functional phenotypes during inflammation and recovery. During inflammation, most macrophages are an M1 phenotype; then, they switch to an M2 phenotype during recovery. Simultaneously, the mechanical environment is actively changing, with extracellular matrix (ECM) degradation in the inflammation phase and ECM regeneration and remodeling in the recovery phase. However, how these dynamic mechanical cues affect macrophage phenotype is unknown.

In the present study, I demonstrated the effect of AKAP12+ colon mesenchymal cells on macrophage phenotypes during dextran sodium sulphate (DSS)-induced colitis. Contraction of the matrix stimulated by AKAP12 might be attributable to its ability to regulate the mechanical processes of cells, which is evidenced by the observation that AKAP12 KO mice have a loose ECM structure during intestinal inflammation recovery. I also showed that AKAP12 KO mice were more sensitive to DSS-induced colitis than WT mice, as the tissue contraction leads to the generation of M2 macrophages and reduction of the inflammation response during recovery.

MATERIALS AND METHODS

1. Animals

Breeding colonies of WT and AKAP12 KO mice (C57BL/6J background) were established and used for comparison experiments. All mice were maintained in a SPF room in the animal-housing facilities at the Seoul National University. Animal experiments were approved by the Committee for Care and Use of Laboratory Animals at the Seoul National University, according to the Guide for Animal Experiments edited by the Korean Academy for Medical Sciences.

2. Induction and assessment of DSS colitis

Mice were given 2% DSS (molecular weight: 36,000-50,000; MP Biomedicals) in their drinking water, and mice were weighed every 24 h. Colitis severity was assessed by several clinical and histological parameters. Body weight changes and survival rate were shown as mean weight loss to initial body weight and ratio of survived mouse until each day respectively. Other clinical feature such as decreased movements, rectal bleeding, and anaemia were recorded. The length of colon and submucosa was measured after 12 days. Histological features

such as epithelial degeneration, epithelial hyperplasia and submucosa edema were compared by using confocal microscope

3. Tissue harvesting and histology

Anesthetized mice were perfused with 0.1 M PBS (pH 7.4). Tissue samples of colon were prepared by using ‘swiss roll’ method as described previously30. Isolated colons were cleaned by flushing of PBS through internal of colons and opened longitudinally. Then, opened colon was rolled on wooden stick and fixed with 4% PFA at 4 ℃. After dehydration with serial gradients of sucrose, the colons were embedded in OCT compound (Sakura) and 10-μm-thick colon cryosections were made for immunofluorescence staining.

4. Immunofluorescence

Colon frozen sections and collagen sections were blocked in staining solution (1% BSA, 0.5% triton in PBS) and incubated with primary antibodies against AKAP12 (I. Gelman, Roswell Park Cancer Institute), Fibronectin, α-smooth muscle actin (DAKO), Collagen I, Collagen III, Raldh2 (Abcam), CD11b, F4/80 (AbD Serotec), iNOS (BD), Arginase I (Santa cruz), Vinculin, (Sigma), PDGFRa (R&D

systems), PGP9.5 (Ultraclone) and phalloidin (Molecular Probes) at RT 1h followed by Alexa 488, 546 and 350 (Invitrogen) secondary antibodies at RT for 1 h. Nuclear-staining was performed with Hoechst 33342 (Molecular Probes). Images were obtained with confocal microscopy (Carl Zeiss, LSM700)..

5. Primary culture of colon mesenchymal cells (CMCs) and macrophages

For isolation of CMCs, colons from 6–10 week old WT or AKAP12KO mice were dissected, cut in 2-3 mm pieces and washed with HBSS without calcium and magnesium ion (Invitrogen). To remove the epithelial layer, intestinal pieces were then incubated in the HBSS containing 5 mM EDTA and 1 mM DTT for 20 min in shaking incubator at 37℃ two or three times. After chopped by scissors, incubated with 1mg/ml Collagenase D (Roche), 1 mg/ml Dispase II (Sigma-aldrich) and 25U/ml DNase I (Sigma-aldrich) in DMEM (Gendepot) for 60 min in shaking incubator at 37℃ twice. Supernatants were centrifuged and cell pellets were resuspended in DMEM supplemented with 10% FBS (Gendepot), 100U/ml penicillin, 100μg/ml streptomycin and 0.25μg/ml amphotericin B and plated in

cell culture flasks. The cells at passages 2-3 were used. Bone-marrow derived macrophages (BMDMs) were gained similar to described previously (Weischenfeldt and Porse, 2008). Briefly, femur and tibia were obtained from 8–12 week old WT or AKAP12 KO C57BL/6 mice. After sacrifying the mouse by cervical dislocation, hind legs of the mouse were dissected and skin and muscle of the leg were removed by using sterile scissors and forceps. In a sterilized condition, epiphyses were removed and the bones flushed with 20ml ice-cold sterile PBS by 22-gauge needle syringe through 70μm strainer (BD falcon) into 50ml tube. Filtrates were centrifuged at 500g and supernatants discarded. Pellets resuspended in RPMI (Gendepot), supplemented with 10% FBS, 100U/ml penicillin, 100μg/ml streptomycin and 0.25μg/ml amphotericin B, plated in cell culture flasks. After 4-6 h incubation at 37℃, supernatants were collected and resuspended in complete RPMI containing 30% L929 conditioned media. Resupended cell suspension filtered through 40μm strainer plated on petri dish and differentiated at 37℃ for 5 days.

6. Collagen gel assay

Collagen type I purified from rat tail (Corning) was used to

fabricate three dimensional matrix. Collagen gels were formed by collagen fibril self-assembly inside of 24-well culture plate. Briefly, the pH of the collagen type I solution was adjusted to 7.4 by mixing with 1M NaOH, NaHCO3, H2O, 10xRPMI (Sigma Aldrich) and cell suspension. And the collagen solutions were incubated at 37℃ for 30 minutes. After gelation, RPMI were added into collagen gels. After 6 h, gels were released by using fine straight and curved forceps to promote cell based remodelling of matrix. Gels were incubated for 2 d and used for further analysis.

For immunofluorescence, collagen gel matrices remodelled by CMCs were fixed with 4% PFA, dehydrated with sucrose, embedded in OCT compound and sectioned in 10-μm-thick tissue.

7. Flow cytometry

For isolation of colon lamina propria mononuclear cells, procedures were same as described in primary culture of CMCs and macrophages until digesting colon lamina propria to dissociate cells from the tissues. Then mononuclear cell population was selected from the cell suspension by using percoll gradient separation. Dissociated cells were resuspended to 40% percoll solution layered up to 80%

percoll solution. Resuspension were centrifuged at 1000g at 20℃ without brakes. Carefully collected cells in interphase of layered solutions were washed once with FACS buffer (3% BSA in PBS).

For isolation of cells in collagen gels, these were digested with digestion solution containing 1mg/ml Collagenase D (Roche), 1 mg/ml Dispase II (Sigma-aldrich) and 25U/ml DNase I (Sigma-aldrich) for 1hr at 37℃ in shaking incubator and repeated once. Supernatants were centrifuged at 500g and washed once with FACS buffer

These suspensions were blocked with mouse CD16/CD32 antibodies for 30 minutes at 4℃ and stained with V450-conjugated antibodies to mouse CD11b, PE-conjugated antibodies to mouse F4/80, APC-conjugated antibodies to CD206 (Biolegend) for 1hr at 4℃. Then, washed with FACS buffer and analyzed. Samples were acquired with FACSVerse (BD Bioscience) and data were analyzed with FACSuite software.

8. Mechanical properties of collagen gels

The mechanical properties of the collagen gels matrix were characterized with Advanced Rheometric Expansion System (ARES). Collagen gels inserted with colon primary mesenchymal cell were

remodelled for two days and fixed with 4% PFA. And then the mechanical properties were then measured similar method to previous report (Chaudhuri et al., 2014). The storage modulus at 1% strain and at 1Hz was recorded periodically until the storage modulus reached its equilibrium value (~10min). Then, a strain sweep was performed to confirm this value was within the linear elastic regime.

9. RNA isolation and qRT–PCR

Total RNA isolation of colon tissue was performed by using Tissue lyser II (Qiagen) and TRIZOL reagent (Invitrogen). Isolated RNA was quantified with a NanoDrop ND-1000 spectrophotometer and cDNA was synthesized by M-MLV reverse transcriptase (Promega). Colon tissue from DSS induced mice further purified by method of lithium chloride purification. For qPCR, reactions were run on a real-time PCR system (Step One Plus; Applied Biosystems) and gene expression was detected with SYBR Green (Enzynomics). Relative gene expression was determined by normalizing to reference genes GAPDH, using the comparative threshold cycle (CT) method. Results were expressed as fold change of each sample versus control. The primers used in each reaction were as follows : CXCR4 forward 5’-

AAAGCTAGCCGTGATCCTCA-3’ and reverse 5’-CACCATTTCAGGCTTTGGTT-3’; CD206 forward 5’-GCTGAATCCCAGAAATTCCGC-3’ and reverse 5’-ATCACAGGCATACAGGGTGAC-3’ ; GAPDH forward 5’-GGGTGAGGCCGGTGCTGAGTATG-3’ and reverse 5’-GGCAGAAGGGGCGGAGATGATG-3’. Statistical data analyses were performed using a two-tailed unpaired Student’s t-test between any two groups (n=4).

10. Western blotting

The cells used were homogenized and lysed in buffer [20 mM Tris-HCl (pH 7.5), 150 mM NaCl, 1 mM Na2EDTA, 1 mM EGTA, 1% Triton, 2.5 mM sodium pyrophosphate, 1 mM beta-glycerophosphate, 1 mM Na3VO4, 1 μg/ml leupeptin, and protease inhibitor cocktail. Immunoblotting was performed using primary antibodies against AKAP12 (Santa Cruz, I. Gelman, Roswell Park Cancer Institute), α-tubulin (BioGenex).For triton soluble/insoluble fractionation, cells were treated with MG132, a proteasome inhibitor, for 3 h, then lysed in a PBS buffer containing 1% Triton X-100 and a protease inhibitor cocktail. After sonication, cells were centrifuged

for 30 min at 100,000×g in 4℃. The soluble fractions were used in western blot analysis for the detection of ubiqutinated proteins.

11. Enzyme-linked immunosorbent assay

CMCs and LPS (100ng/ml) primed BMDMs or LPS primed BMDMs alone (control) were co-cultured in collagen gels for 2 days and culture supernatant was assayed for TNF-α by using Mouse TNF-α ELISA MAX standard sets (Biolegend) in coating 96-well plates (Corning). TNF-α concentration was calculated from standard curve. Results were presented as fold change versus control.

12. Bioinformatics

Publicly available datasets of ulcerative colitis patients and DSS induced colitis mouse gene expression microarrays were downloaded from the GEO database (http://www.ncbi.nlm.nih.gov/geo: GSE38713 and GSE22307) and re-analyzed. The expression profiles of AKAP12 and MRC1 were extracted from the independent datasets, then quantitative preparing of AKAP12 in each groups were performed and the relationship between the expression of AKAP12 and MRC1 was determined by correlation analysis. Differentially expressed genes

in groups of ulcerative colitis patients and DSS-induced colitis were detected and ranked by using GEO2R software in pubmed. Then, genes significantly changed ($P<0.001$) were functionally categorized according to KEGG pathway using DAVID 6.7 software and the biological processes related with AKAP12 protein function were selected. Significantly correlated genes clusters with AKAP12 ($R>0.8$) were also classified with KEGG pathway.

13. Data analysis and statistics

Statistical analysis was done with an unpaired two-tailed Student's t test. Results with a P value of <0.05 were considered statistically significant. Data are represented as the means ± S.E.M. Pearson's coefficients with associated P-values were used for correlation analysis.

RESULTS

1. AKAP12 is highly expressed in colon mesenchymal cells and regulates ECM

AKAP12 was highly expressed in both normal and inflamed mouse colons which were induced by ingestion of DSS (Figure 10). The expression of AKAP12 was not observed in α-smooth muscle actin (α-SMA) positive mesenchymal cells, but no in myeloid cells (Figure 11) (Powell et al., 2011). Because these cells function as organizers of the tissue matrix (Hinz and Gabbiani, 2003), it prompted us to compare the ECM structure in the colon environment of WT and AKAP12 KO mice. Indeed, the collagen and fibronectin structures differed in the mucosa of inflamed colons of WT and AKAP12 KO littermates (Figure 12A, B); shortened and tightened ECM structures were observed in WT mucosa, whereas linear and longer structures were observed in AKAP12 KO mucosa. The mucosa of AKAP12 KO normal colons even showed a small aberration in the fibronectin structure and the submucosa of AKAP12 KO colon is slightly longer than that of WT

colon (Figure 13). Moreover, in whole colon primary cultures, the collagen structure derived from AKAP12 KO mice was not connected (Figure 14), and the fibronectin structure in the AKAP12 KO culture was larger than that in the WT culture (Figure 15). These results imply that AKAP12 + CMCs have effect on ECM organization.

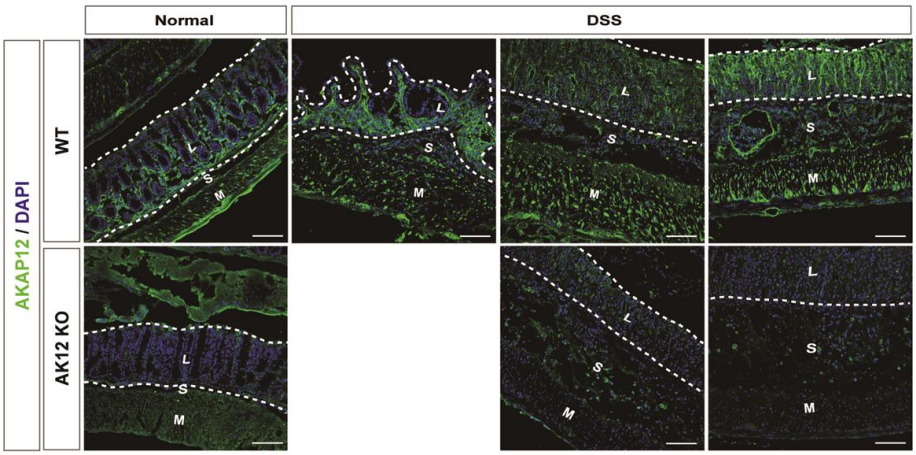

Figure 10. AKAP12 is highly expressed in both normal and inflamed colon. Normal colon tissue and DSS-induced colitis colon tissue of WT and AKAP12 KO mice were immunostained with antibody against AKAP12 and nuclei were counterstained with DAPI. L: lamina propria (Mucosa), S: submucosa, M: muscularis externa. Scale bars: 100 μm.

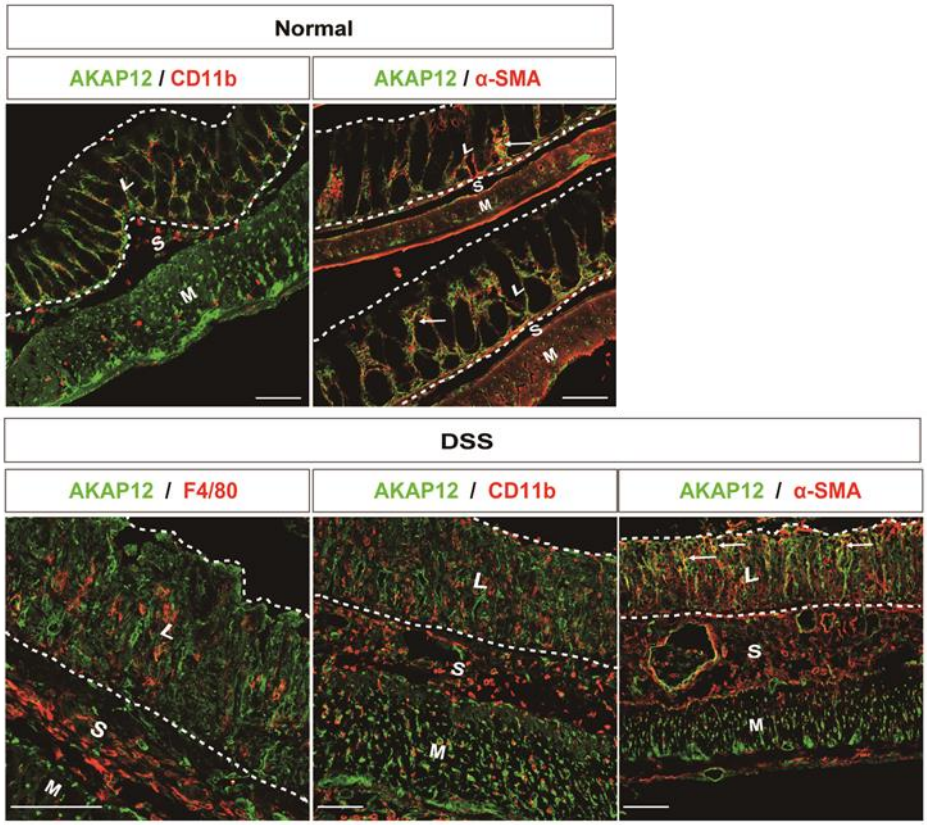

Figure 11. The cell type expressing AKAP12 under both normal and inflamed colon. AKAP12 was expressed in α-SMA positive mesenchymal cells, not in myeloid cells. Normal colon tissue and DSS-induced colitis colon tissue of WT and AKAP12 KO mice were immunostained with antibodies against AKAP12, F4/80, CD11b and α-SMA. L: lamina propria (Mucosa), S: submucosa, M: muscularis externa. Scale bars: 100 μm.

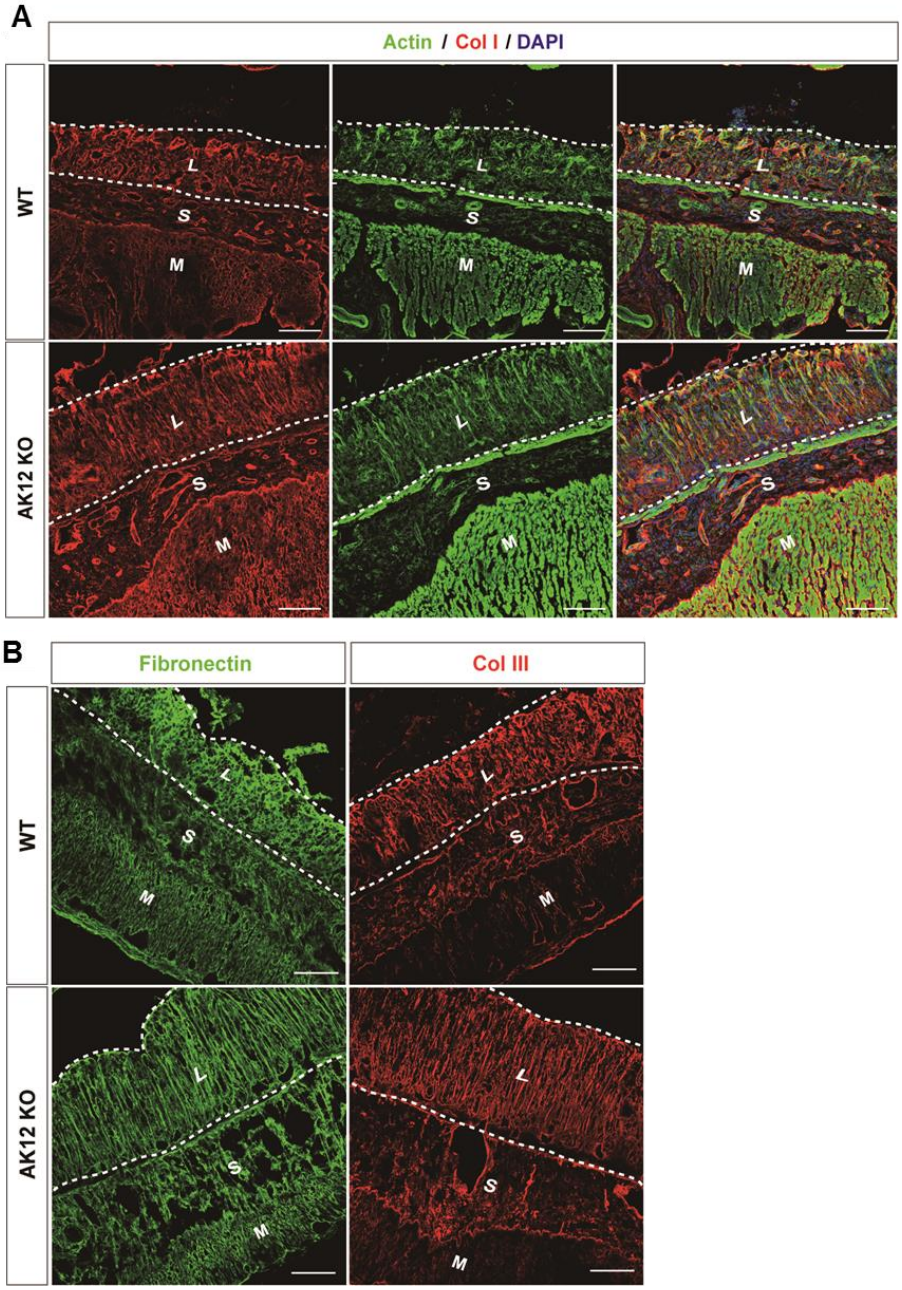
A
Actin / Col I / DAPI
WT
AK12 KO
L
S
M
B
Fibronectin
Col III
WT
AK12 KO
L
S
M

Figure 12. Difference of ECM structures between inflamed colon mucosa of WT and AKAP12 KO mice. WT and AKAP12 KO mice were given 2% DSS in their drinking water for 8 days and were then allowed to recover with normal drinking water for a further 4 days. (A) Colon sections were immunostained with antbody against collagen I and stained with phalloidin for actin and DAPI for nuclei. (B) Colon sections were immunostained with antbodies against collagen III and fibronectin. L: lamina propria (Mucosa), S: submucosa, M: muscularis externa. Scale bars: 100 μm.

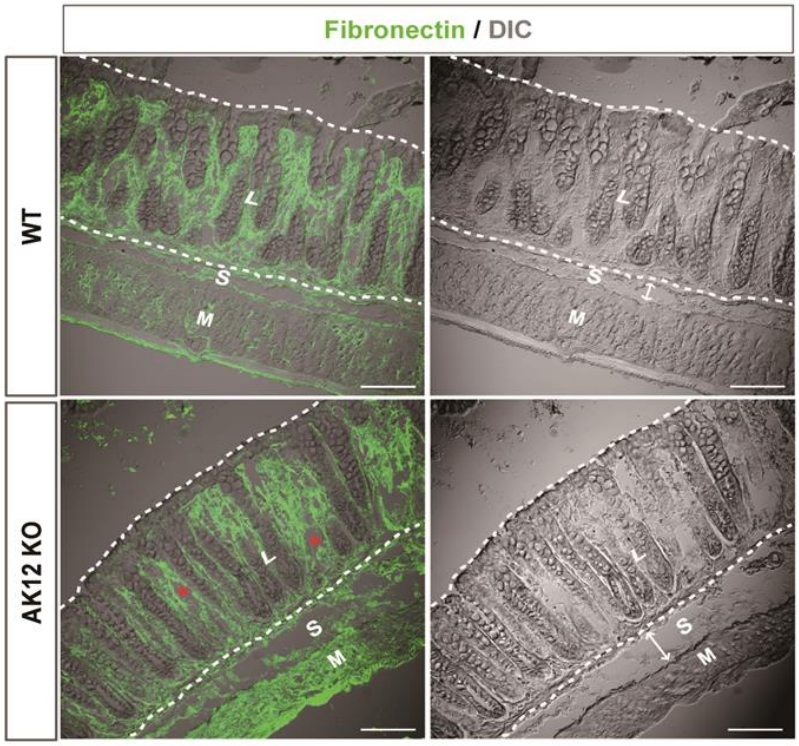

Figure 13. Fibronectin structure in normal colon of WT and AKAP12 KO mice. Colon sections were immunostained with antbody against fibronectin. Small aberrations in colon mucsoa of AKAP12 KO mice are marked by red asterisk and width of submucosa are indicated by bidirectional arrows. L: lamina propria (Mucosa), S: submucosa, M: muscularis externa. Scale bars: 100 μm.

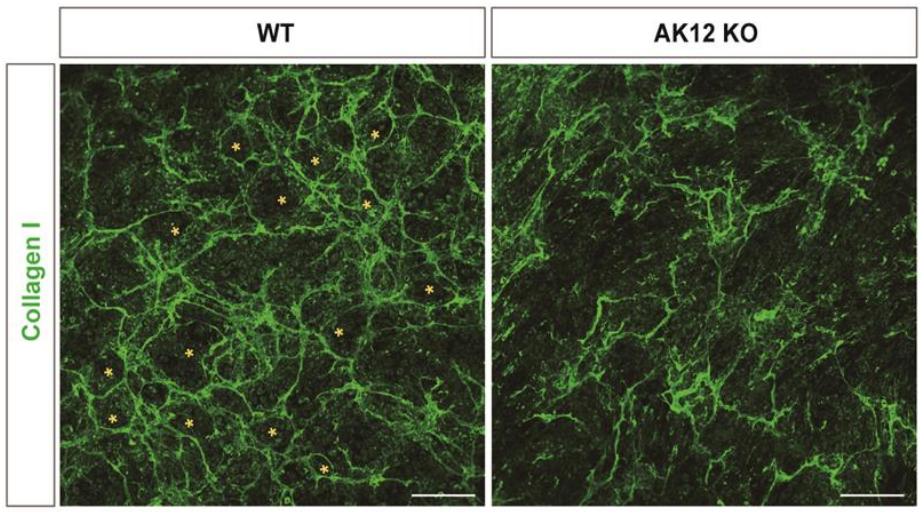

Figure 14. Collagen ring structures were broken in primary culture of AKAP12 KO colon cells. Colon epithelial cells were denuded and the remainder cells were cultured on dish during a week. After the cells were fully packed in dish, collagen I was immunostained with antibody. Collagen ring structures were marked by yellow asterisk. Scale bars: 300 μm.

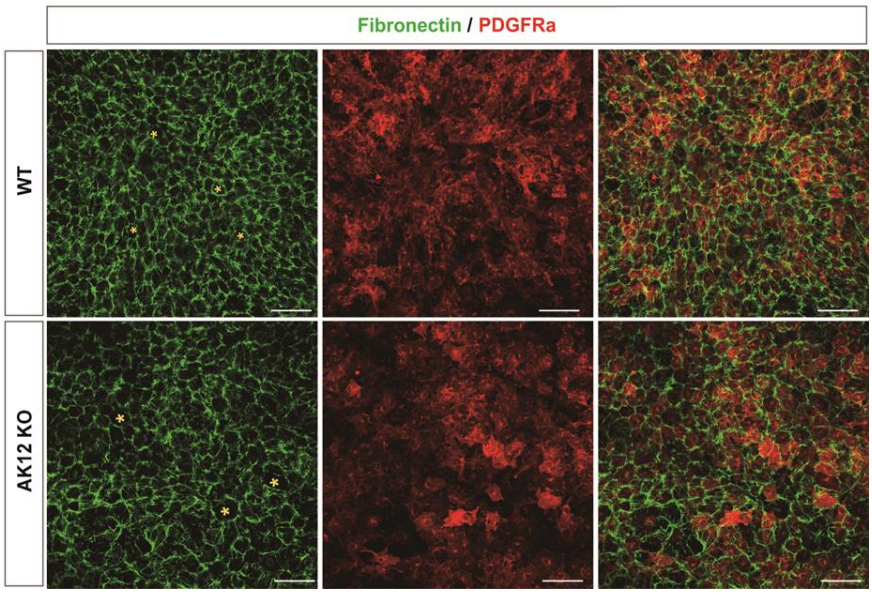

Figure 15. Fibronectin structures were larger in primary culture of AKAP12 KO colon cells than in WT colon cells. Colon epithelial cells were denuded and the remainder cells were cultured on dish during a week. After the cells were fully packed in dish, Fibronectin and PDGFRα were immunostained with antibody. Fibronectin structures were marked by yellow asterisk. Scale bars: 100 μm.

2. Tightness of ECM that is regulated by AKAP12 determines the shape of macrophages

Since the inflammation in the DSS-induced colitis model occurs continuously at colon mucosa, the tissue states are heterogeneous. Therefore, several states of recovering colon mucosa could be seen concurrently. Based on the grade of ECM contraction, I subdivided the structures of inflamed colon mucosa into ‘pre-contracted’, ‘less-contracted’ and ‘contracted’ structures (Figure 16). The expression of AKAP12 was higher in the contracted area than in the less-contracted area (Figure 17). The shape of macrophages was altered under these different structures, implying that mechanical environment may affect the macrophage shape (Figure 16). Interestingly, a contracted structure with ramified macrophages was only observed in WT colons, while pre-contracted and less-contracted structures with round macrophages were observed in both WT and AKAP12 KO colons (Figure 18A, B and 19). Then, I analyzed the properties of contracted and less contracted area. Less-contracted mucosa in AKAP12 KO showed longer height, higher proportion of collagen negative area and lower cell density than contracted mucosa in WT (Figure 20-22), which could be the result of

difficulty on tissue contraction in inflamed colon of AKAP12 KO. These data indicate that AKAP12-mediated contraction of ECM structures promotes the formation of ramified macrophages rather than round macrophages (Figure 23).

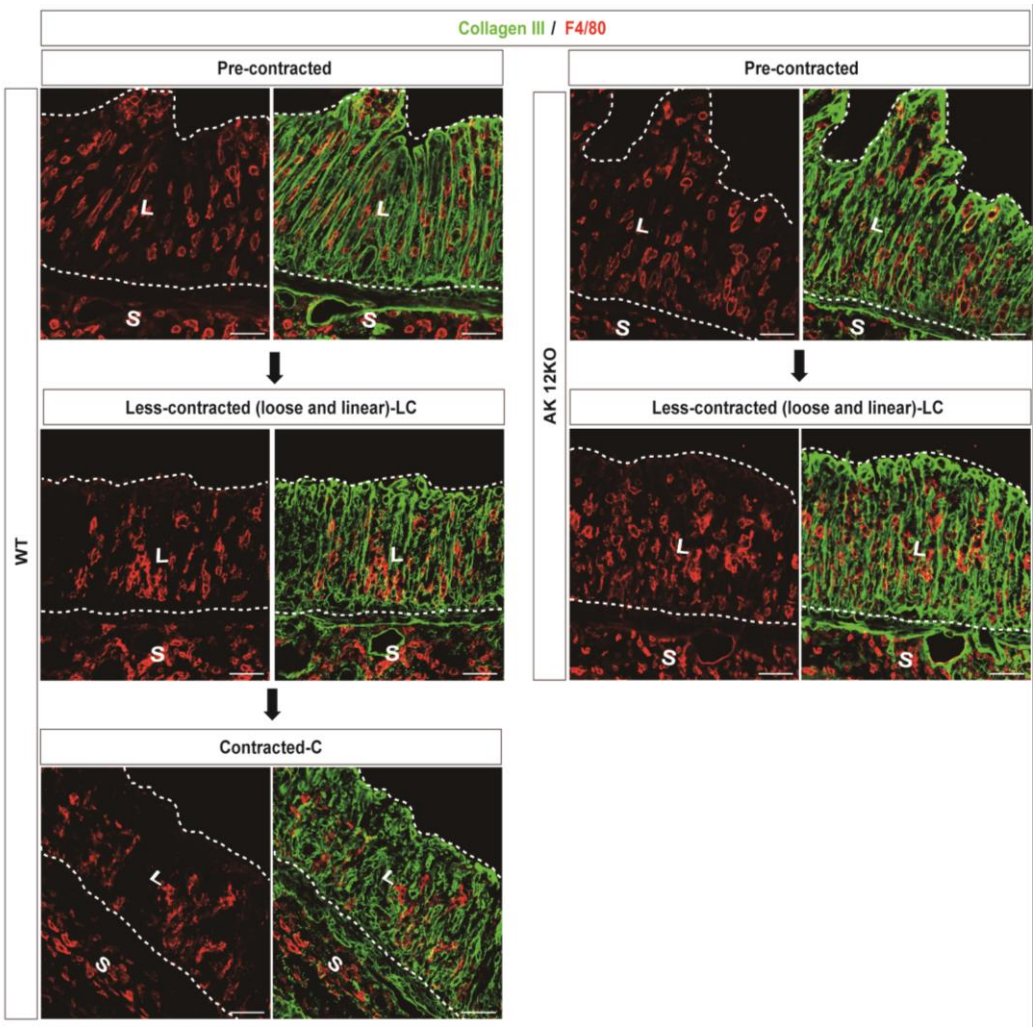
Collagen III / F4/80
Pre-contracted
Pre-contracted
WT
AK 12KO
Less-contracted (loose and linear)-LC
Less-contracted (loose and linear)-LC
Contracted-C
L
S

Figure 16. AKAP12 meditaed contraction of the colon tissue was connected to macrophage shapes. WT and AKAP12 KO mice were given 2% DSS in their drinking water for 8 days and were then allowed to recover with normal drinking water for a further 4 days. Colon sections were immunostained with antbody against collagen III and F4/80. Pre-contracted, less-contracted and contracted areas were selected according to state of collagen structure. L: lamina propria (Mucosa), S: submucosa. Scale bars: 50 μm.

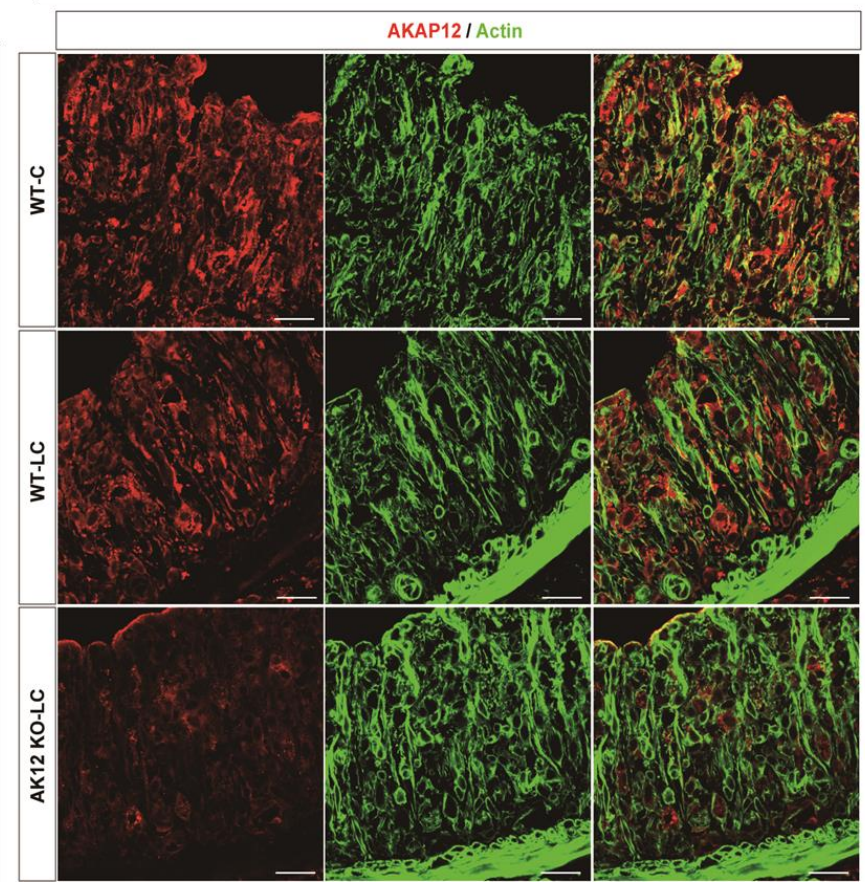

Figure 17. AKAP12 expression was high in contracted mucsoa and low in less-contracted mucsoa. WT and AKAP12 KO mice were given % DSS in their drinking water for 8 days and were then allowed to recover with normal drinking water for a further 4 days. Colon sections were immunostained with antbody against AKAP12 and stained with phalloidin for actin. Scale bars: 25 μm.

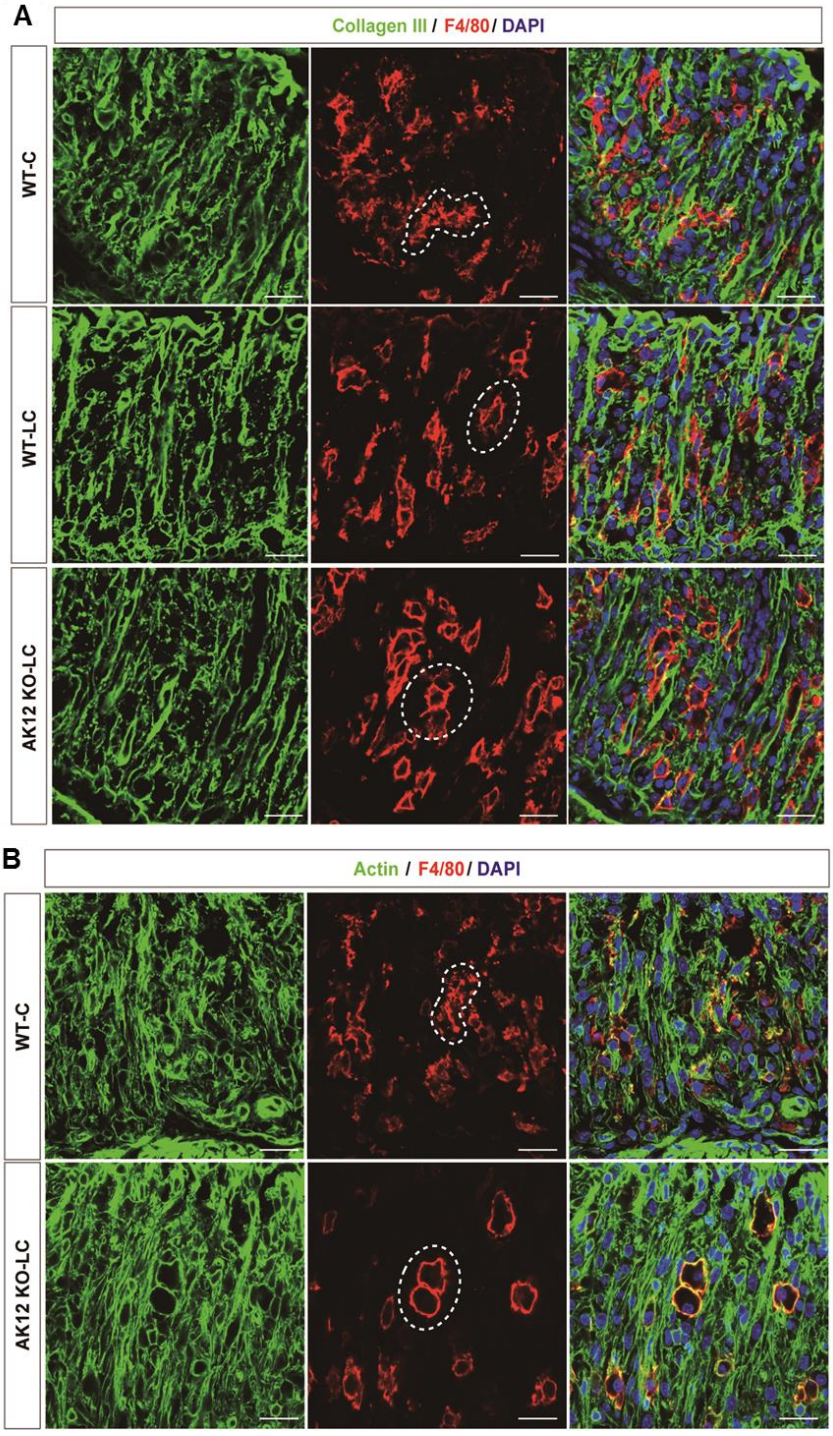
A
Collagen III / F4/80 / DAPI
WT-C
WT-LC
AK12 KO-LC
B
Actin / F4/80 / DAPI
WT-C
AK12 KO-LC

Figure 18. Contracted structure generates ramified macrophages during recovery. WT and AKAP12 KO mice were given 2% DSS in their drinking water for 8 days and were then allowed to recover with normal drinking water for a further 4 days. Colon sections were immunostained with antbodies against Collagen III and F4/80 and stained with phalloidin for actin and nuclei were counterstained with DAPI. The shape of macrophages was marked by dotted line. Scale bars: 25 μm.

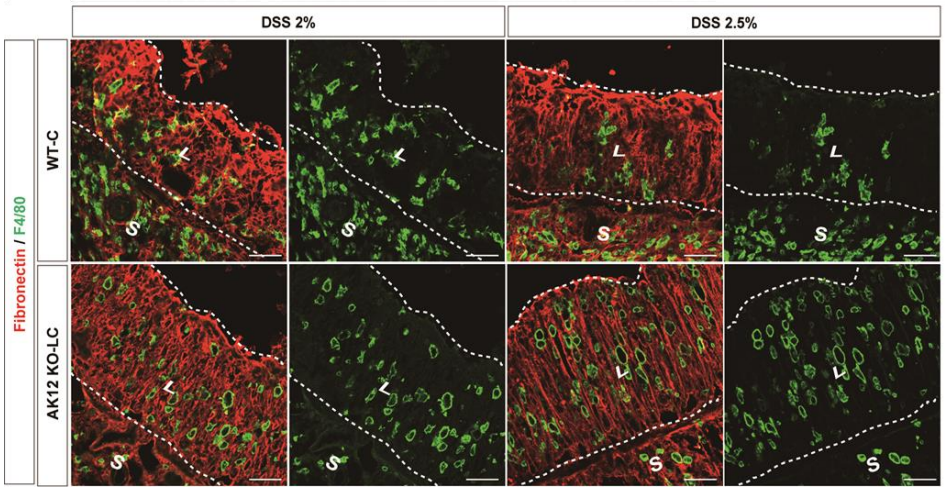

Figure 19. Contracted structure generates ramified macrophages irrespective of DSS concentration. WT and AKAP12 KO mice were given 2% DSS in their drinking water for 8 days and were then allowed to recover with normal drinking water for a further 4 days. Colon sections were immunostained with antbodies against fibronectin and F4/80. L: lamina propria (Mucosa), S: submucosa. Scale bars: 50 μm.

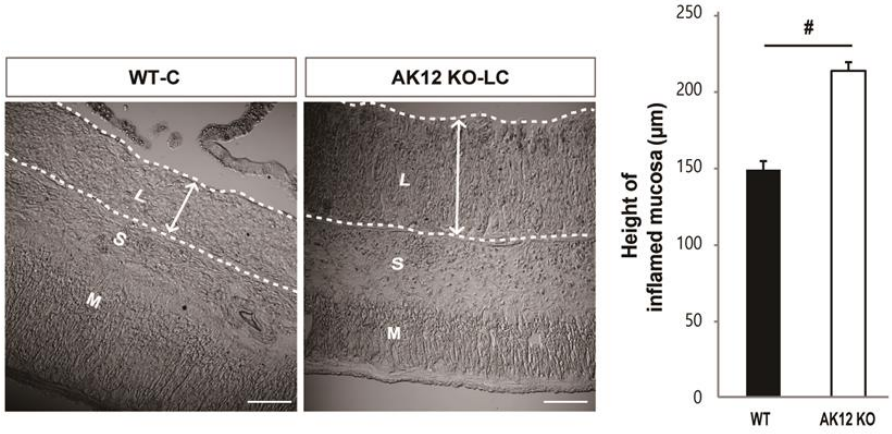

Figure 20. The length of inflamed mucosa is longer in AKAP12 KO mice thn in WT mice. Average vertical height of inflamed mucosa were measured. L: lamina propria (Mucosa), S: submucosa, M: muscularis externa. Scale bars: 100 μm. (n=9 or 7 mice for WT or AKAP12 KO, respectively, mean of 3 different sections used, mean±S.E.M, an unpaired two-tailed Student t-test : $P^{\#}<10^{-4}$).

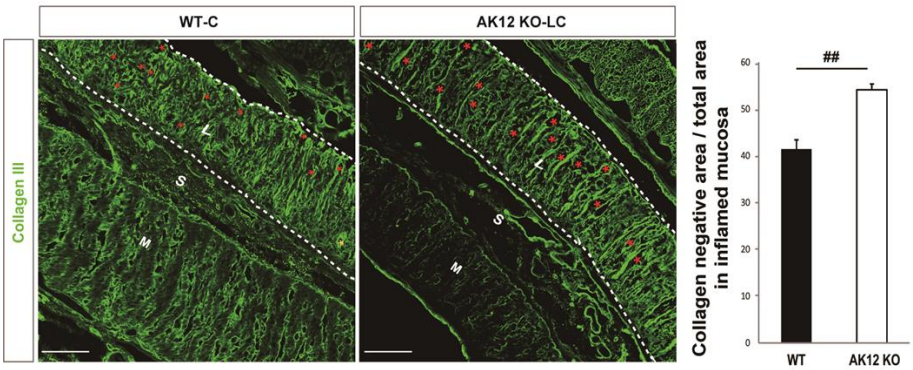

Figure 21. The porosity of inflamed mucosa is higher in AKAP12 KO mice thn in WT mice. Proportion of collagen negative area to total area in mucosa was measured. Hollow pores in WT and AKAP12KO collagen structures were marked by red asterisk of different size L: lamina propria (Mucosa), S: submucosa, M: muscularis externa. Scale bars: 100 μm. (n=6 per group, mean of 2 technical replicates used, mean±S.E.M, an unpaired two-tailed Student t-test : $P^{\#\#}<10^{-6}$).

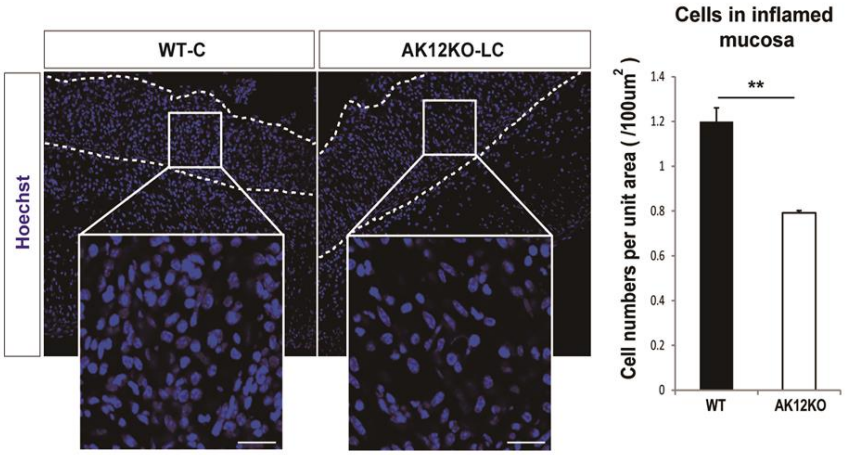

Figure 22. Cell density of inflamed mucosa is lower in AKAP12 KO mice thn in WT mice. Density of cells in inflamed mucosa wasmeasured. Scale bars: 20 μm. Scale bar: 20 μm. (n=7 or 5 for WT or AKAP12KO, respectively, mean of 2 different sections used, mean±S.E.M, an unpaired two-tailed Student t-test : $P^{**}<10^{-2}$)

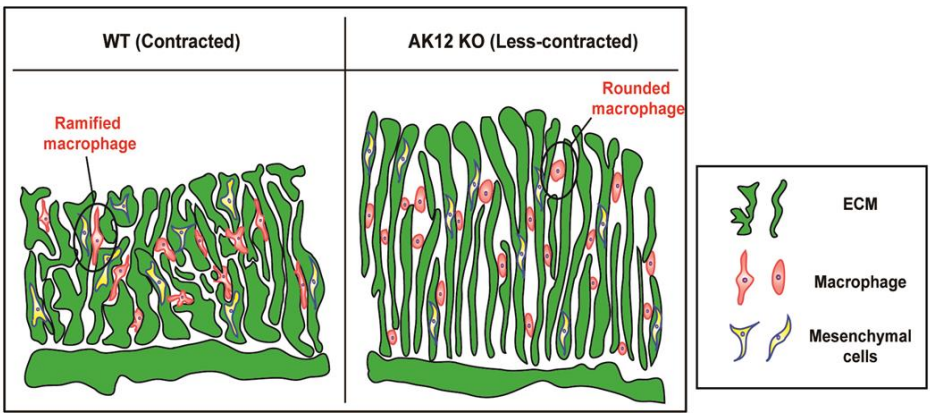

Figure 23. Schematic representation of ECM structure and macrophage shapes in WT and AKAP12 KO inflamed mucsoa. Ramified macrophages present in contracted structures and round macrophages in less-contracted structures were marked by black circle. Less-contracted areas were observed in both inflamed colons of WT and AKAP12 KO mice. However contracted areas were mainly observed in WT inflamed mucsoa, indicating contribution of AKAP12 in tissue contraction.

3. Tissue contraction by AKAP12+ CMCs drives the ramified M2 macrophage

Alterations in the cell shape have long been associated with changes in cell function (Folkman and Moscona, 1978). In addition, ramified or elongated macrophages were reported to polarize to M2 phenotypes (McWhorter et al., 2013). Therefore, to determine the relationship between macrophage shapes and their functional phenotypes, I examined the several macrophage markers in each mechanical environment. Interestingly, the proportion of arginase I+ macrophages, stands for M2 macrophage, was higher in the contracted area with ramified macrophages than in the less-contracted area with round macrophages. In contrast, the population of inflammatory macrophages marked by iNOS was higher in the less-contracted area than in the contracted area (Figure 24 and 25). In addition, round macrophages in the less-contracted inflamed mucosa showed higher expression of ninjurin1, an inflammatory macrophage marker (Ahn et al., 2014), than ramified macrophages in the contracted inflamed mucosa (Figure 26).

Therefore, the population of arginase I+ M2 macrophages was lower and that of iNOS+ and ninjurin1+ inflammatory macrophages were

higher in AKAP12 KO inflamed mucosa than in WT (Figure 27). The proportion of CD206+ M2 macrophages among the total macrophages was also higher in WT inflamed colons than in AKAP12 KO ones (Figure 28 and 29). In addition, the relative expression of tumor necrosis factor-α (TNF- α), a pro-inflammatory cytokine, was higher in AKAP12 KO inflamed colon and the population of interleukin-10 (IL-10)+ cells, an anti-inflammatory cytokine, was lower in AKAP12 KO inflamed colons (Figure 30). Level of M2 macrophage markers and related cytokine were also lower in AKAP12 KO colons under normal conditions (Figure 31). Collectively, these data show that the contracted tissue drives anti-inflammatory environment by generating ramified M2 macrophages.

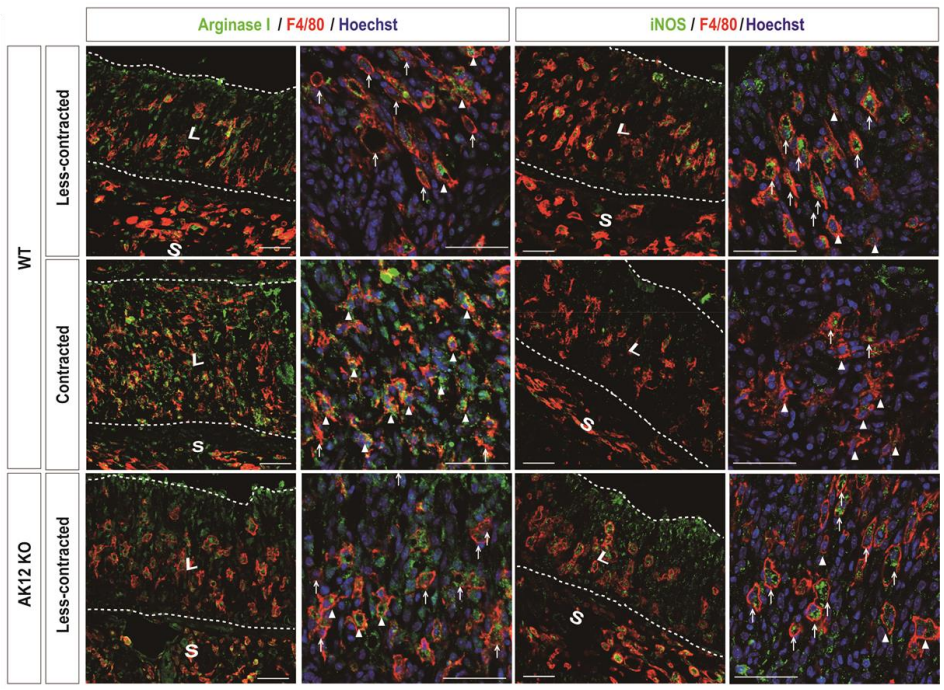
Arginase I / F4/80 / Hoechst
iNOS / F4/80 / Hoechst
WT
AK12 KO
Less-contracted
Contracted
Less-contracted
L
S

Figure 24. Ramified macrophages in contracted structures polarize to M2 macrophages. WT and AKAP12 KO mice were given 2% DSS in their drinking water for 8 days and were then allowed to recover with normal drinking water for a further 4 days. Colon sections were immunostained with antbodies against arginase I, iNOS and F4/80 and nuclei were counterstained with Hoechst33342. Less-contracted and contracted mucosa was selected according to macrophage shapes. Arg1+ macrophages and Arg1- macrophages are marked by arrowheads and arrows, respectively. iNOS+ macrophages and iNOS- macrophages are marked by arrows and arrowheads, respectively. Scale bars: 50 μm.

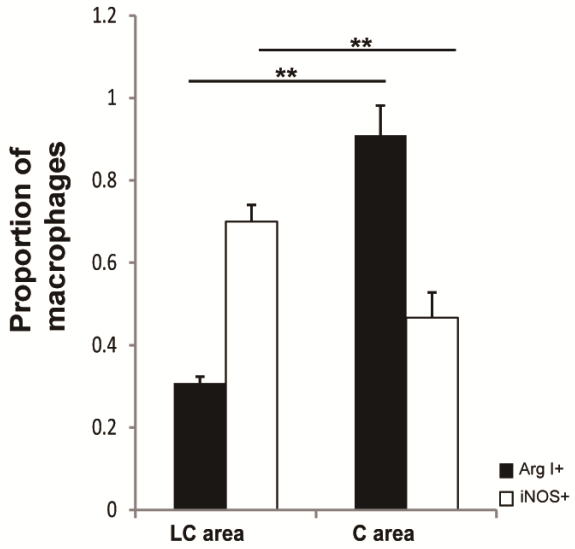

Figure 25. The proportions of M1 or M2 macrophages in contracted or less contracted structures. Proportions of arginase I and iNOS positive macrophages to total macrophages in less-contracted and contracted mucosa of WT mice were calculated (n=3 per all group, mean±S.E.M, an unpaired two-tailed Student t-test : $P^{**}<10^{-2}$).

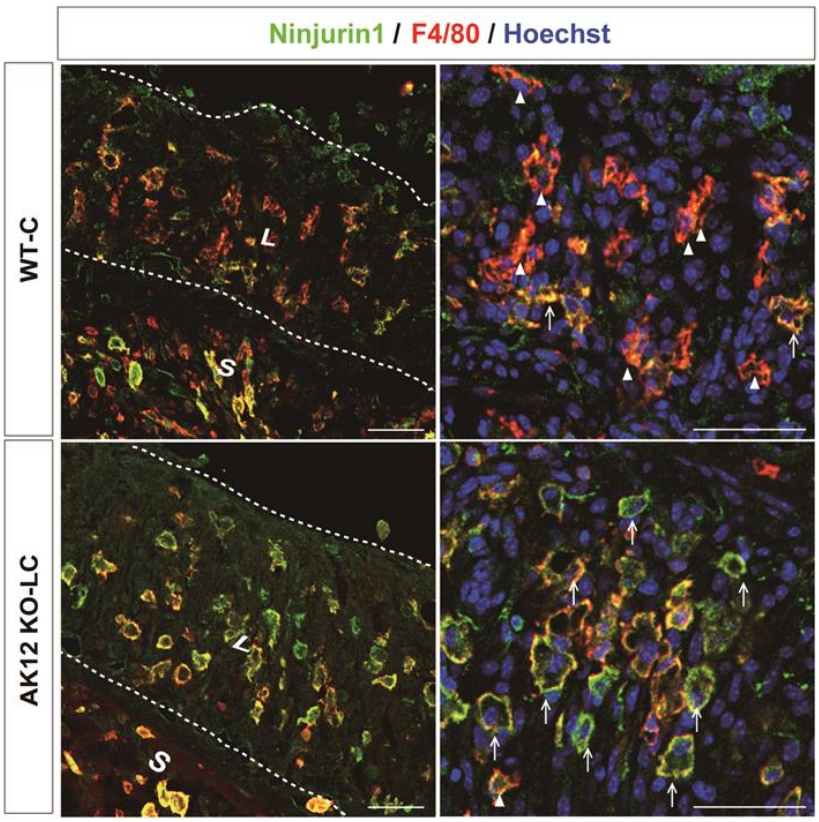

Figure 26. The expresson of Ninjurin1 was higher in round macrophages than in ramified macropahges. WT and AKAP12 KO mice were given 2% DSS in their drinking water for 8 days and were then allowed to recover with normal drinking water for a further 4 days. Colon sections were immunostained with antbodies against Ninjurin1 and F4/80 and nuclei were counterstained with Hoechst33342. Ninjurin 1+ macrophages and Ninjurin1- macrophages are marked by arrows and arrowheads, respectively. Scale bars: 50 μm.

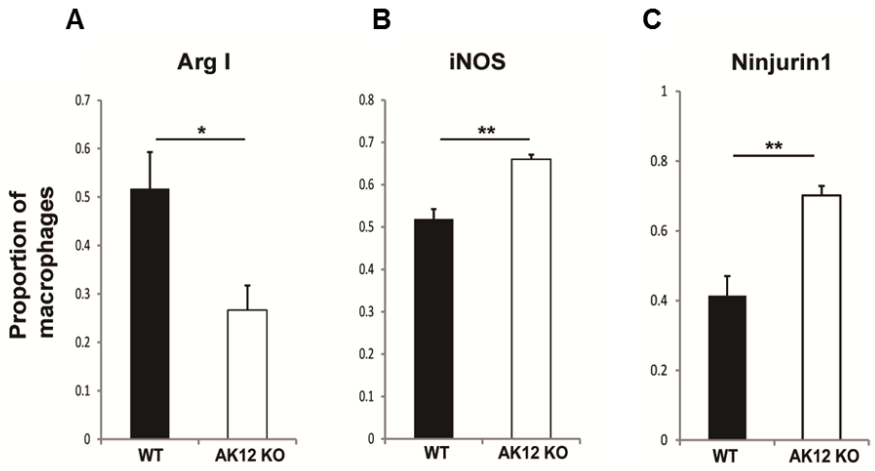

Figure 27. The proportions of anti-inflammatory or inflammatory macrophages in inflamed colon mucosa of WT and AKAP12 KO mice. Proportions of arginase I+ and iNOS+ macrophages to total macrophages in WT and AKAP12 KO inflamed mucosa were calculated. (n=4 for iNOS+ and Ninjurin1 in AKAP12 KO inflamed mucosa, n=3 per all rest group, mean±S.E.M, an unpaired two-tailed Student t-test : $P^{**}<10^{-2}$, $P^{*}<0.05$).

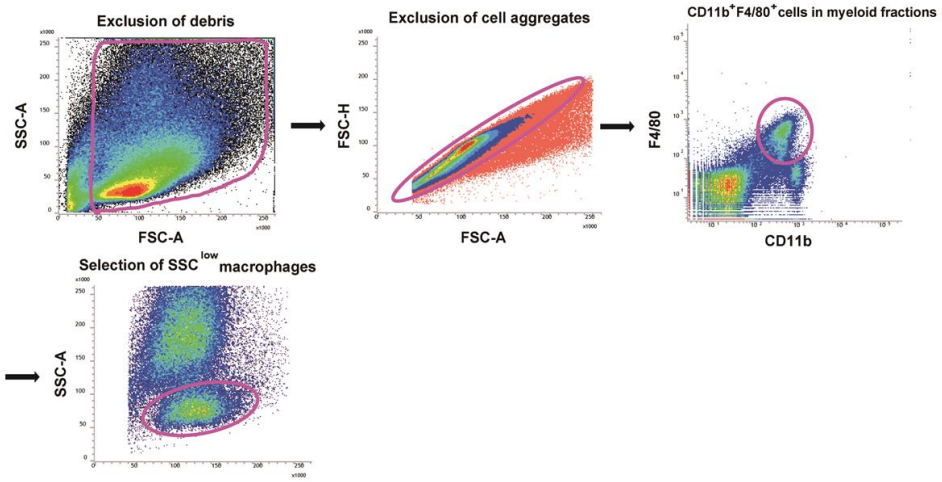

Figure 28. Gating strategy for isolating the macrophage population in DSS-induced mouse colons. Cells in pink circle are gated. First, whole prepared cell populations were gated. Then, singlets of the cells were gated. CD11b+ F4/80+ cell included the macrophages and eosinophils. Macrophages were selected by SSC

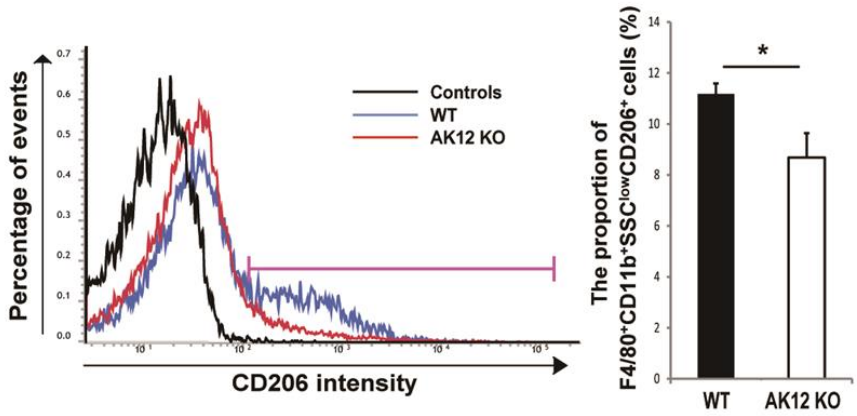

Figure 29. Proportion of M2 macrophage is higher in colitis-induced colons of WT mice than that of AKAP12 KO mice. Representative FACS plot for CD206 positive macrophages in WT and AKAP12 KO inflamed colon. Macrophages within pink bars were considered as M2 macrophages. CD206-negative controls are shown in black (n=4 per group, mean±S.E.M, an unpaired two-tailed Student t-test: $P^{*}<0.05$)

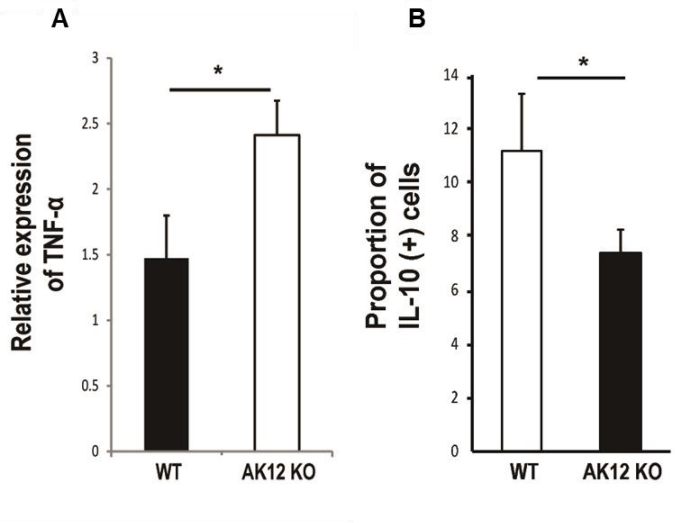

Figure 30. Inflammatory cytokine is higher and anti-inflammatory cytokine is lower in AKAP12 KO inflamed colons than in WT inflamed colons. TNFα mRNA expression in WT and AKAP12 KO inflamed colon were detected by Real-time PCR and IL-10 positive cells were measured by FACS. (n=4 per group, mean±S.E.M, an unpaired two-tailed Student t-test: $P^{*}<0.05$)

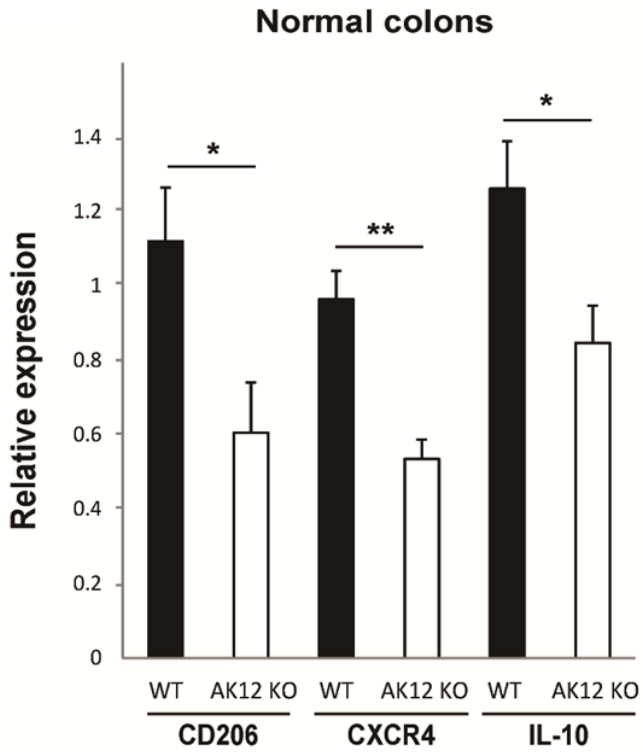

Figure 31. Expression of M2 macrophage markers is lower in normal colons of AKAP12 mice than in that of WT mice. CD206, CXCR4 and IL-10 mRNA expression in WT and AKAP12 KO normal colon were detected by Real-time PCR (n=4 per group, mean±S.E.M, an unpaired two-tailed Student t-test: $P^{**}<10^{-2,}$ $P^{*}<0.05$)

4. AKAP12 KO shows the increased sensitivity to DSS-induced colitis

Next, I compared the clinical symptoms of colitis in WT and AKAP12 KO mice to determine whether differences in the mechanical environment are correlated with the severity of intestinal inflammation. Mice ingested 2% or 2.5% DSS in water for 8 days, and then fresh water for 4 days. (Figure 32) There was no obvious difference in water consumption (Figure 33). The clinical symptoms were more severe in AKAP12 KO mice, mirrored by greater weight loss, lower survival, more blood in stools (Figure 34A-C). In addition, repetitive DSS-induced colitis experiments confirmed that AKAP12 KO mice were more sensitive to colitis in most experiments. Colon length, which indicates the degree of colon damage, was also shorter in colitis-induced AKAP12 KO mice than in WT mice, whereas it was similar in both genotypes under normal conditions (Figure 35). Epithelial degeneration and mucosal hyperplasia were only observed in WT inflamed mucosa and the average width of the submucosa that shows degree of submucosal oedema was longer in AKAP12 KO inflamed colon than in WT, implying more severe histological damage in AKAP12 KO inflamed colon than in WT (Figure 36).

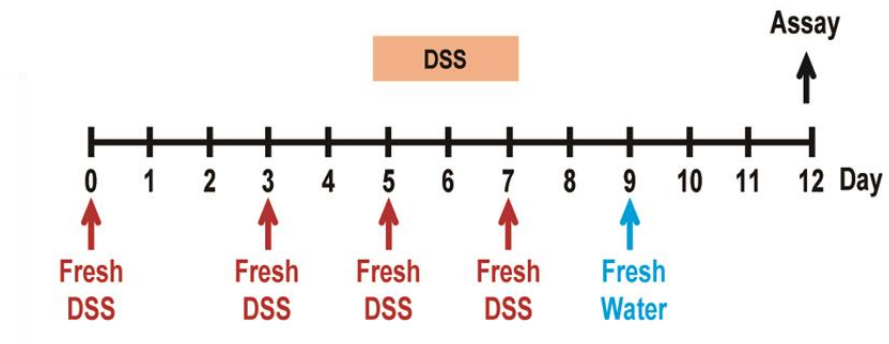

Figure 32. Schedule of DSS ingestion to WT and AKAP12 KO mice. WT and AKAP12 KO mice were given DSS in their drinking water for 8 days and were then allowed to recover with normal drinking water for a further 4 days.

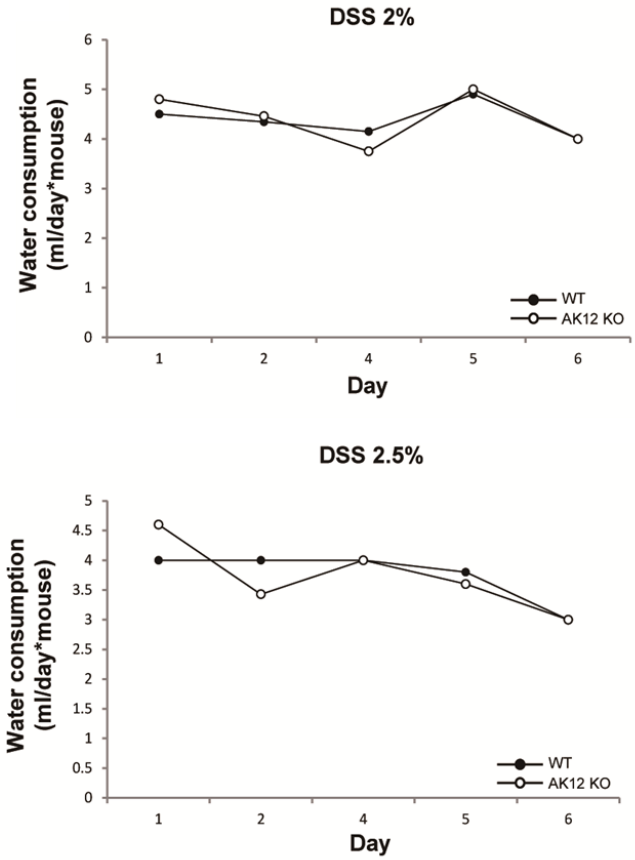

Figure 33. Comparison of consumption of DSS in water by WT and AKAP12 KO mice. Consumption of DSS 2% or 2.5% in water per cage was calculated from diminished volume of water and then divided by number of mouse.

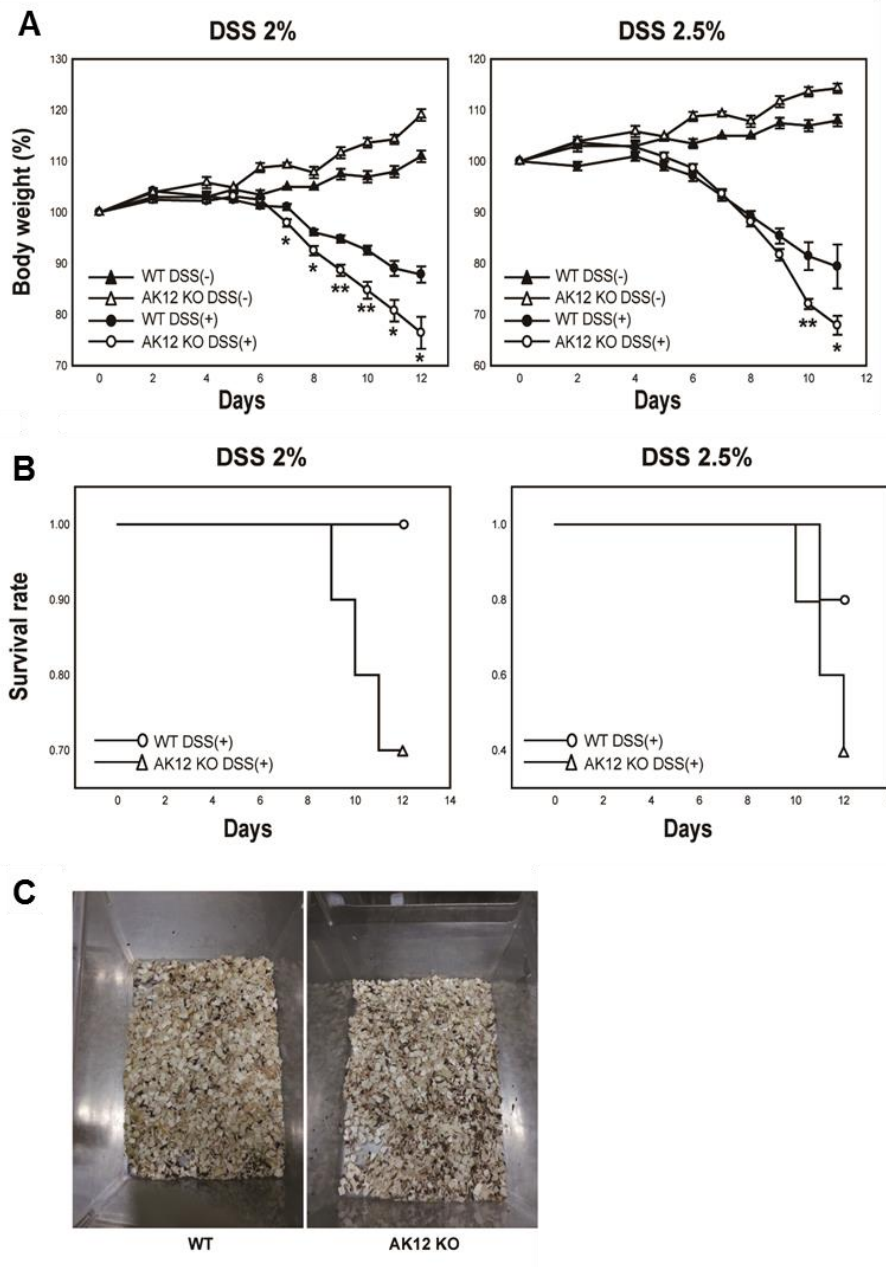
A
DSS 2%
DSS 2.5%
Body weight (%)
Days
WT DSS(-)
AK12 KO DSS(-)
WT DSS(+)
AK12 KO DSS(+)
B
DSS 2%
DSS 2.5%
Survival rate
Days
WT DSS(+)
AK12 KO DSS(+)
C
WT
AK12 KO

Figure 34. Clinical symptoms were more severe in DSS-induced colitic colon of AKAP12 KO mice than in that of WT mice. WT and AKAP12 KO mice were given 2 or 2.5% DSS in their drinking water with control group (normal water) for 8 days and were then allowed to recover with normal drinking water for a further 4 days. (A) Percentage of body weight changes in WT and AKAP12 KO mice after given 2 or 2.5% DSS in water. (B) Proportion of survived mouse to total mouse in each groups were recorded at each days. (C) Blood stools in WT and AKAP12 KO mice cage after induction of colitis. (n=10 for DSS 2% group and n=5 for DSS 2.5% group, mean±S.E.M, an unpaired two-tailed Student t-test: $P^{**}<10^{-2,}$ $P^{*}<0.05$)

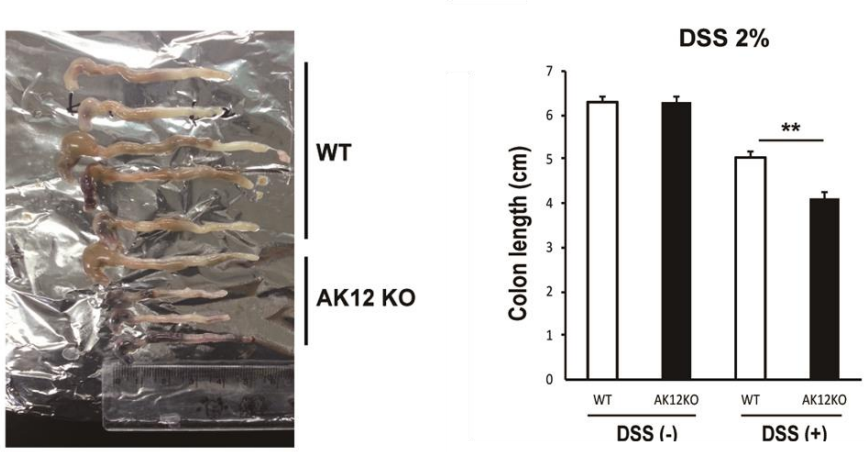

Figure 35. Colon length was shorter in DSS-induced colitic colon of AKAP12 KO mice than in that of WT mice. Colon lengths were recorded by using ruler on day 12 (n=3 for normal WT and AKAP12KO colon and n=5 or 4 for inflamed colon WT or AKAP12KO, respectively, mean±S.E.M, an unpaired two-tailed Student t-test: $P^{**}<10^{-2}$)

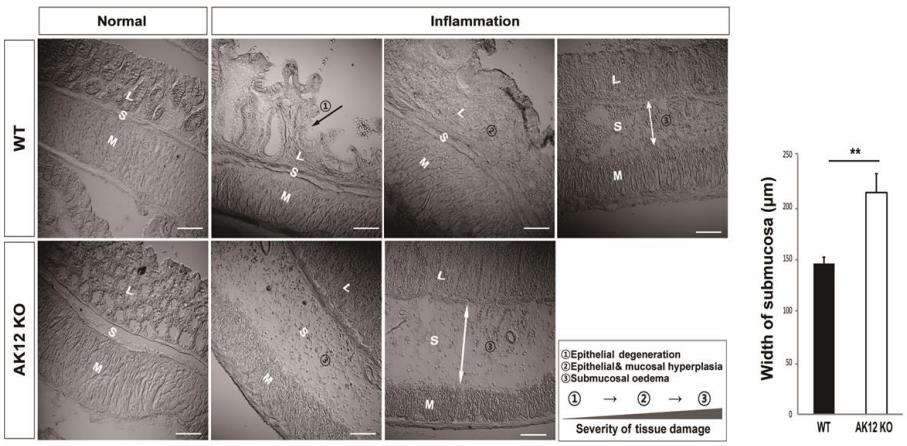

Figure 36. Histological damage was more severe in DSS-induced colitic colon of AKAP12 KO mice than in that of WT mice. Tissue states were marked in images and numbered with order of tissue damage. Width of submucosa in image was measured by ruler and then the value was converted to real value by using scale (n=5 per group, mean±S.E.M, an unpaired two-tailed Student t-test: $P^{**}<10^{-2}$). Scale bars: 100 μm.

5. Protective role of AKAP12 contributes to recovery of inflamed colon

Interestingly, the difference in the body weight changes between WT and AKAP12 KO mice gradually increased in the later phase of colitis, during which tissue healing and contraction might take place in a large portion of the inflamed colon. To identify whether the severe damage in AKAP12 KO mice is caused by reduced the ablity of the recovery, I changed DSS water to fresh water for each mouse when it reached 90% of its initial body weight (Figure 37). When the clinical signs were compared after the time point at which fresh water was supplied, WT mice showed a mild decrease in body weight after 1 day, which was maintained thereafter. In contrast, AKAP12 KO mice showed a continuous decrease in body weight, which was accompanied by a dramatic reduced survival rate (Figure 38). These data show that AKAP12 has a protective role in the tissue remodelling phase of DSS-induced colitis.

.0

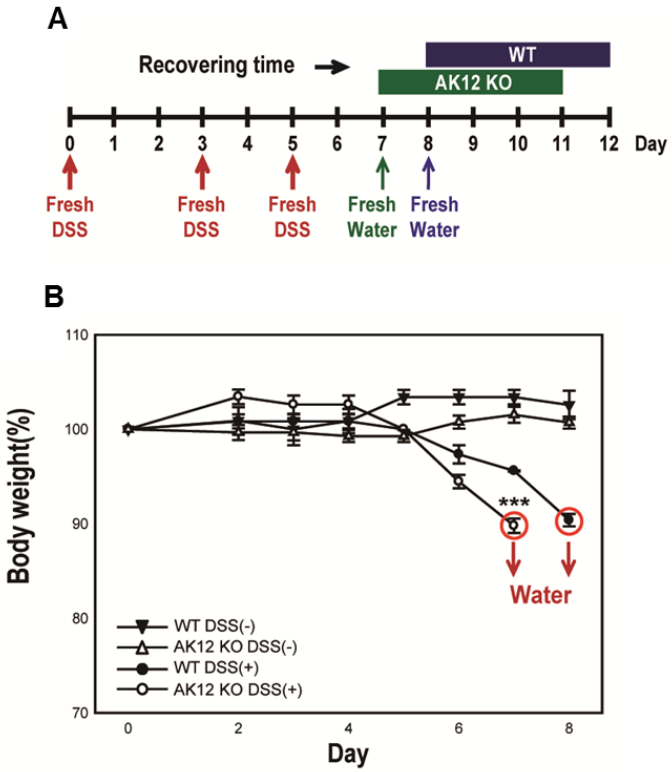

Figure 37. Experimental plan for comparing the accurate recovery ability of inflamed WT and AKAP12 KO colons. WT and AKAP12 KO mice were given normal water for further 4 days after given 2% DSS until body weight of each group decreased to 90% compared to initial body weight or after given normal water (control) (n=5 per group for DSS 2% and n=5 per group for controls). (A) Schedule for comparing the recovering ability of WT and AKAP12 KO mice directly. (B) Body weights of WT and AKAP12 KO were decreased to 90% at 8 day and 7 day, respectively (red circle)

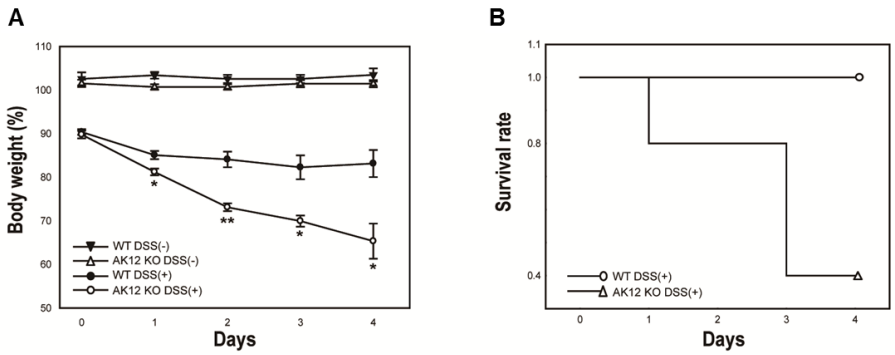

Figure 38. AKAP12 KO mice show reduced ability of intestinal recovery. (A) Body weight changes of WT and AKAP12 KO mice in recovering period were shown. (B) Proportion of survived mouse to total mouse in each groups were recorded at each days. (n=5 per group, mean±S.E.M, an unpaired two-tailed Student t-test: $P^{**}<10^{-2}$, $P^{*}<0.05$)

6. AKAP12 + CMCs promotes collagen gel compaction

Next, to demonstrate that the phenomenon is caused by AKAP12+ mesenchymal cells, not by either a difference in the degree of inflammation or the macrophage itself, I designed an in vitro experiment to assess the macrophage polarity in different mechanical environments. As the remodelling of collagen gel mimics tissue contraction, it is an appropriate model to verify our in vivo results. First, I gained the primary colon-derived mesenchymal cell (pCMCs) from WT and AKAP12 KO colon and then allowed to pCMCs to remodel the collagen gel (Figure 39). Similar with in vivo results, collagen gels remodelled by WT pCMCs (WT pCMCs-gel) highly expressed AKAP12 (Figure 40) and showed more dense and compacted structures than collagen gels remodelled by AKAP12 KO pCMCs (AKAP12 KO pCMCs-gel) (Figure 41 and 42) I also observed that collagen gels remodelled by WT pCMCs were actually stiffer than gels remodelled by AKAP12 KO pCMCs (Figure 43 and 44).

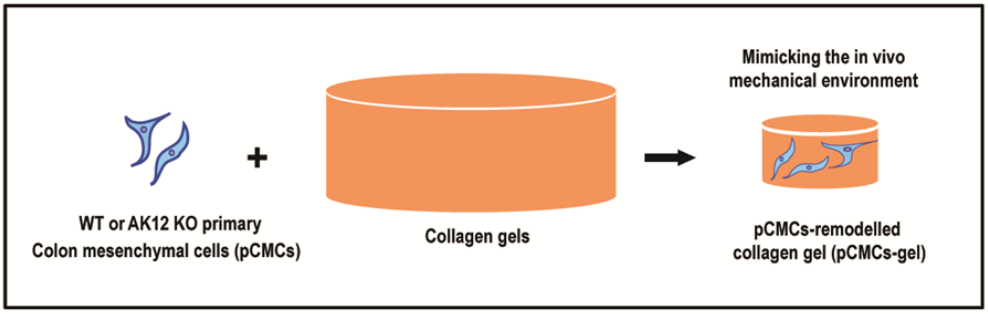

Figure 39. Experimental design of collagen gel remodelling by WT or AKAP12 KO primary colon mesenchymal cells (pCMCs). To establish pCMCs-gel, $7x10^5$ WT or AKAP12 KO pCMCs were inserted in 3mg/ml collagen gels, released from plate after incubated during 8 hr and then further incubated until 48 hr.

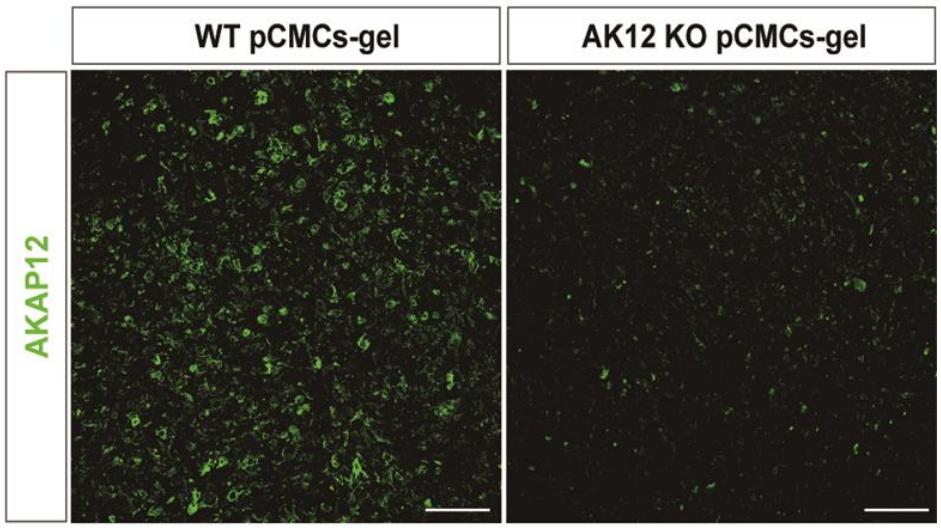

Figure 40. AKAP12 is highly expressed in pCMCs-gel. Collagen gels remodelled by WT or AKAP12 KO pCMCs were fixed and sectioned. WT or AKAP12 KO collagen gels were then immunostained with antibody against AKAP12. Sacle bars: 100 μm

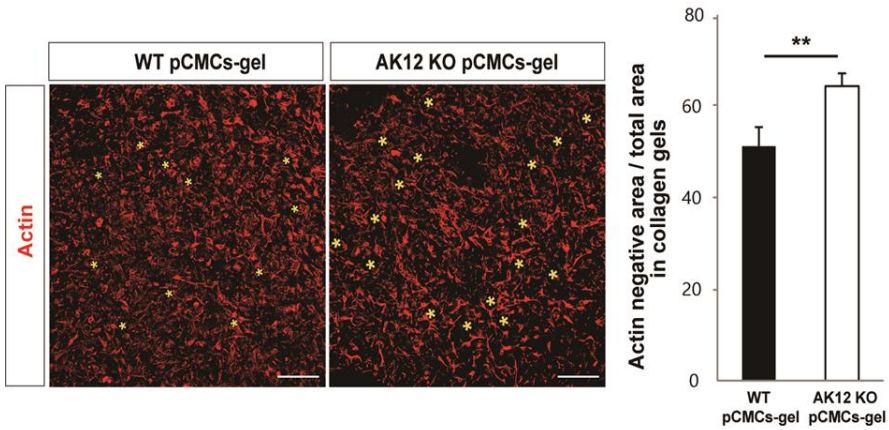

Figure 41. The porosity of actin was higher in AKAP12 KO pCMCs-gel than in WT pCMCs-gel. Actins in collagen gel were stained with phalloidin. Actin negative area to total area of WT pCMCs and AKAP12 KO pCMCs-gels with was measured. Actin-negative area in representative images of each gels were marked by yellow asterisk with different size. Scale bars: 100 μm. (n=3 per group, mean±S.E.M, an unpaired two-tailed Student t-test: $P^{**}<10^{-2}$)

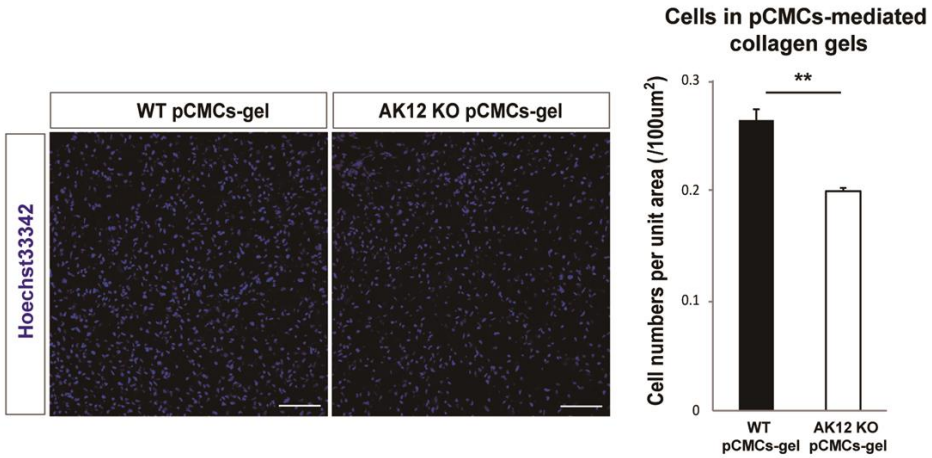

Figure 42. The cell density was lower in AKAP12 KO pCMCs-gel than in WT pCMC-s gel. Cell nuclei in collagen gel were counterstained with Hoechst33342. Density of cells in collagen gels per each group were measured by calculate the number of cells per area. Scale bars: 100 μm. (n=3 per group, mean±S.E.M, an unpaired two-tailed Student t-test: $P^{**}<10^{-2}$)

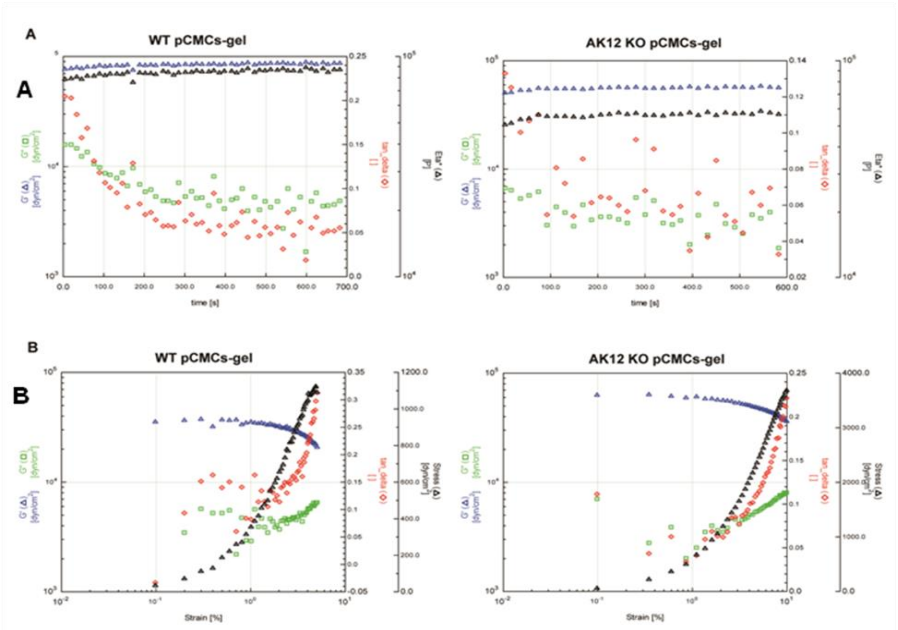

Figure 43. Measurement of the stiffness of remodelled collagen gels.

(A) Representative chart of periodically modulus in WT and AKAP12 KO pCMCs mediated collagen gels. (B) Representative chart of recorded modulus versus strain in WT and AKAP12 KO pCMCs-gels.

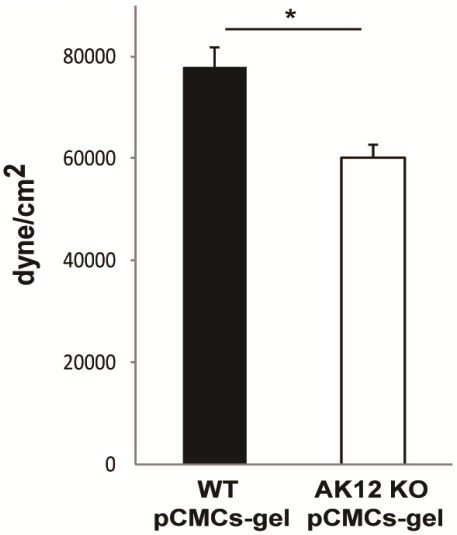

Figure 44. Collagen gels remodeled by WT pCMCs is stiffer than the gels remodeled by AKAP12 KO pCMCs. The storage modulus at 1% strain and at 1Hz of fixed WT and AKAP12 KO pCMCs-gels were averaged. (n=6 per group, mean±S.E.M, an unpaired two-tailed Student t-test: $P^{*}<0.05$).

7. AKAP12+ pCMCs mediated-gel compaction drives macrophages to deeper M2 side and reduces inflammatory response

To identifying the macrophage polarity in the different mechanical environment, WT or AKAP12 KO bone marrow-derived macrophages (BMDMs) were inserted into two-dimensional (2D) plate, three-dimensional (3D) gel, pCMCs-gel and into 3D gel with pCMCs-gel (Figure 45). In accordance with previous results, AKAP12 expression was not detected in BMDMs, but was detected in pCMCs (Figure 46A) and collagen gels were remodelled by pCMCs, not by BMDMs alone, implying that the difference in macrophage polarity between inflamed colon of WT and AKAP12 KO mice is caused by AKAP12+ CMCs (Figure 46B). After remodelling of collagen gels for 2 days, I isolated the inserted BMDMs and analyzed their CD206 expression (Figure 47). The CD206 expressions levels of WT and AKAP12 KO BMDMs in 2D plate or 3D gels were similar. No significant difference in CD206 expressions of WT and AKAP12 KO BMDMs which were inserted into 3D gel and cultured with WT and AKAP12KO pCMCs-gel, respectively, was also observed. Notably, I found a significant difference in the expression of CD206 in the WT and AKAP12 KO

BMDMs inserted into WT and AKAP12 KO CMCs-gel, respectively (Figure 48A), implying that the difference of mechanical environment, generated by tissue remodelling, promotes the difference in macrophage polarity. Then, to verify that this difference in macrophage polarity is caused by pCMCs rather than BMDMs, I measured CD206 expression of BMDMs in WT or AKAP12 KO pCMCs-gel. CD206 expressions in both WT and AKAP12 KO BMDMs were lower in AKAP12 KO pCMCs-gels than in WT pCMCs-gels (Figure 48B), and, this difference between WT and AKAP12 KO BMDMs was not observed when cultured in 3D gels with WT or AKAP12 KO pCMCs-gel (Figure 49).

In accordance with the *in vivo* results, I examined the shape of each BMDM in the pCMCs-gel. Since *in vitro* differentiated macrophages are already ramified and elongated, I was unable to detect round macrophages in collagen gels. Instead, I found that the areas of each macrophage in the AKAP12 KO pCMCs-gel were larger than those in the WT pCMCs- gel, probably due to the loose matrix structure of gels (Figure 50). In addition, the levels of arginase I expression were higher in BMDMs within WT pCMCs-gels than in those within AKAP12 KO pCMCs-gels (Figure 51). These results show that AKAP12 protein in

mesenchymal cells promotes M2 polarization by building a tight mechanical structure in 3D collagen gels.

To confirm these effects in conditions mimicking inflammation and tissue regeneration, I generated lipopolysaccharide (LPS)-primed BMDMs by treating BMDM with LPS 1 day before mixing with collagen and pCMC. CD206 expression of both LPS-primed WT and AKAP12 KO BMDMs in collagen gels decreased similarly compared to WT or AKAP12 KO BMDMs in the collagen gels. The reduced CD206 expressions of LPS-primed BMDMs were more restored in WT pCMCs-gels than AKAP12 KO pCMCs-gels (Figure 52A). I also tested the CD206 expression of LPS-primed each BMDMs in the two pCMCs-gels. CD206 expressions of BMDMs in WT pCMCs-gels were higher than that in AKAP12 KO pCMCs-gels, regardless of macrophage genotypes (Figure 52B). Furthermore, TNF-α secretion from both WT and AKAP12 KO LPS-primed BMDMs was higher in AKAP12 KO CMCs-gels than in WT CMCs-gels (Figure 53). Taken together, these results indicate that the physical environment built by AKAP12+ pCMCs in collagen gels establishes a less inflammatory environment by skewing macrophages to an M2 phenotype.

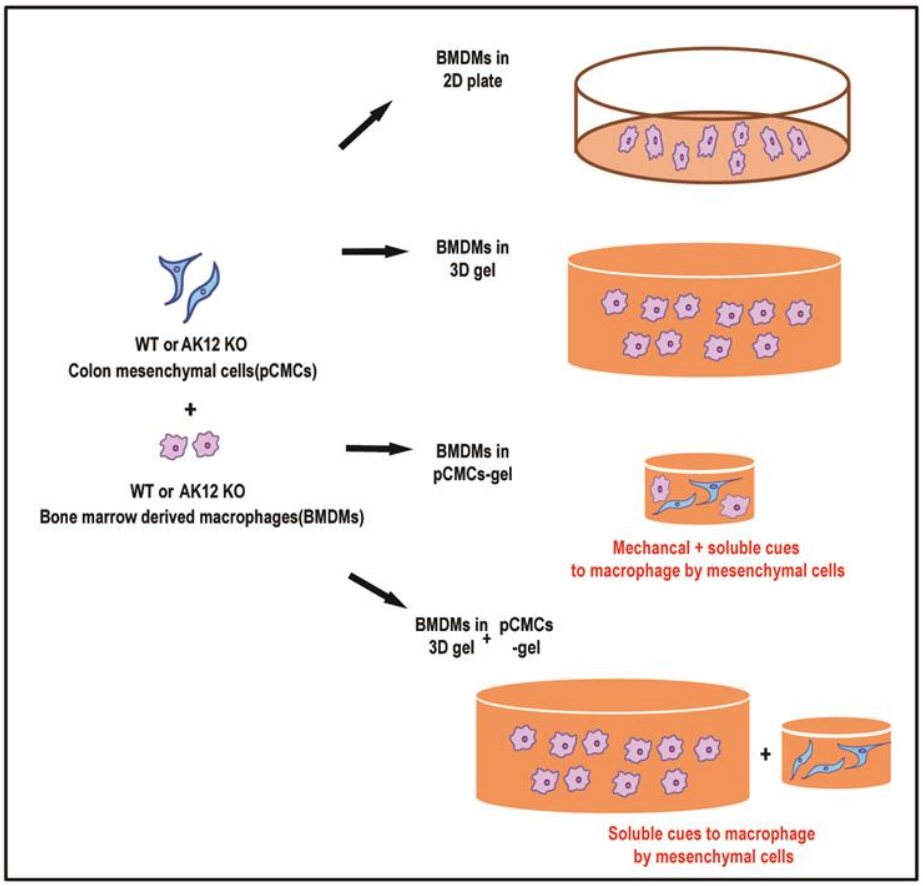

Figure 45. Experimental design of collagen gel assay with pCMCs and BMDMs. $5x10^5$ BMDMs were seeded in 60 mm culture dish, collagen gels, pCMCs-gel or collagen gels with pCMCs-gel. BMDMs were then incubated for 48 hrs in each environment. BMDMs in pCMCs-gel were affected by remodeled gel environment and soluble factors from pCMCs. BMDMs in collagen gel with pCMCs-gel were affected only by soluble factors from pCMCs

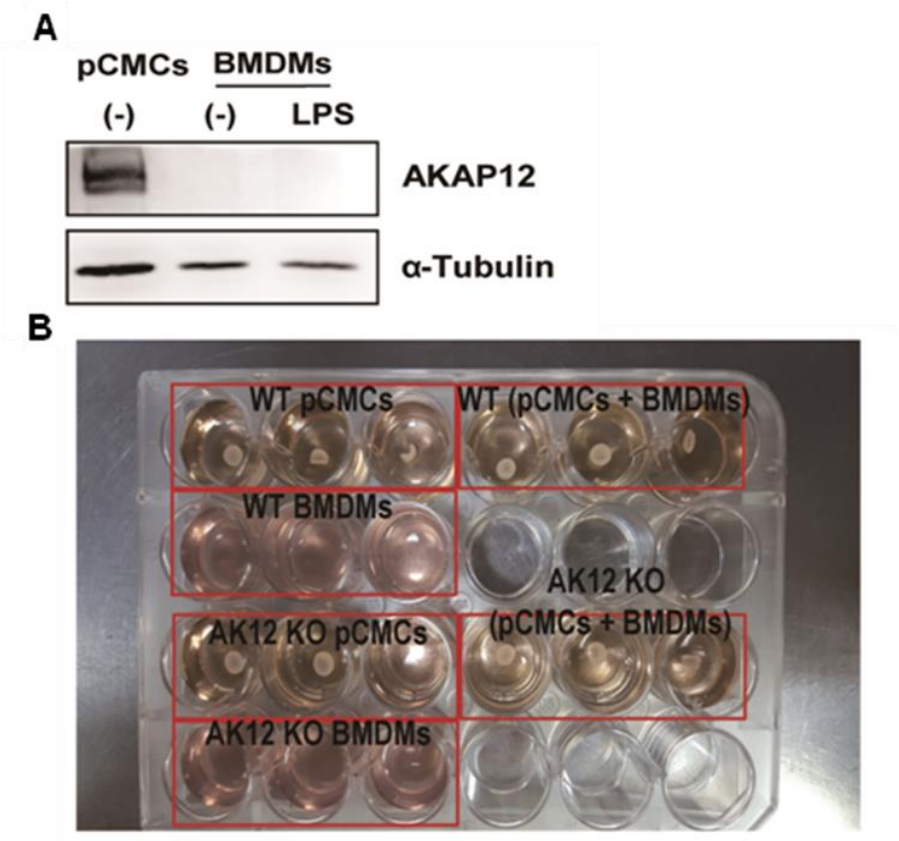

Figure 46. AKAP12 is only expressed in colon mesenchymal cells, not in bone marrow derived macropaghes and collagen gel is remodeled only by colon mesenchyml cells. (A) Immunoblots of AKAP12 and α-tubulin in lysate of WT pCMCs and BMDMs with none or LPS stimulated. (B) Pictures of WT and AKAP12 KO pCMCs, MPs and pCMCs+MPs gels after incubating 48 hr.

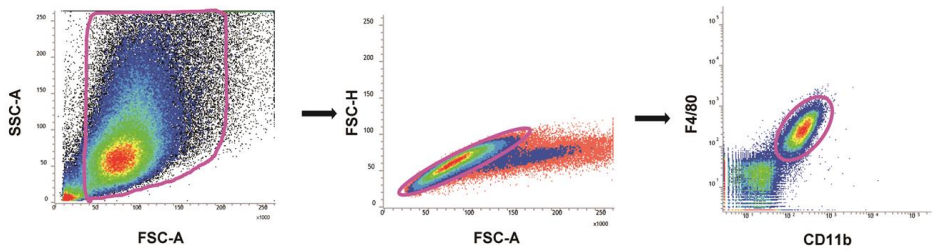

Figure 47. Gating strategy for isolating inserted BMDMs in pCMCs-gels. Cells in pink circle were gated. F4/80+ CD11b+ macrophages were gated.

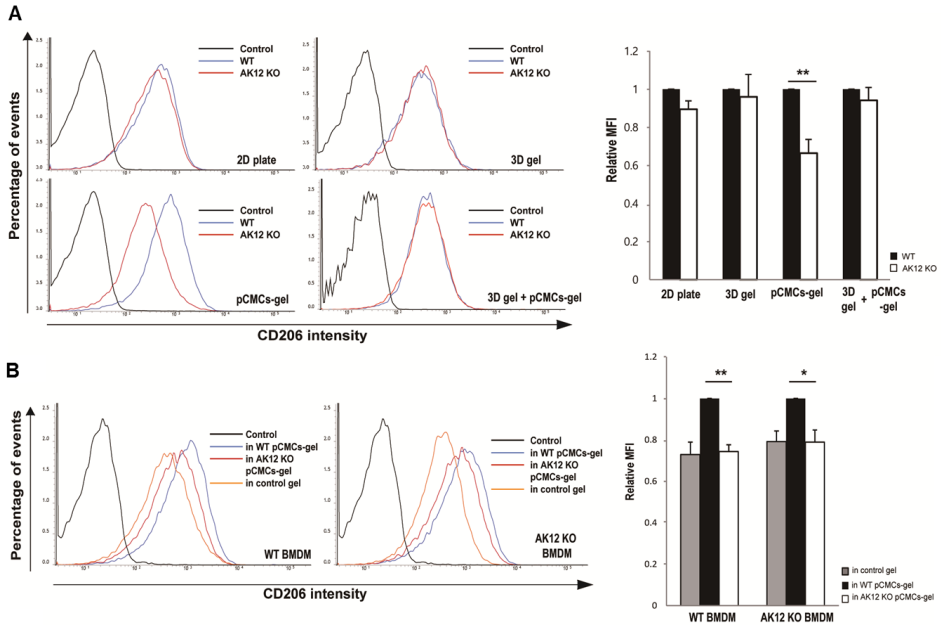

Figure 48. AKAP12-meditaed remodelled gels promote M2 polarization. (A) Representative FACS plots of CD206 stained WT (blue) and AKAP12 KO (red) MPs in 2D plate, 3D gel, pCMCs-gel and 3D gel with pCMCs-gel. CD206-negative controls are shown in black. CD206 fluorescence intensities of BMDMs are normalized to WT BMDMs of each group (n=3, n=6, n=7 and n=3, respectively,

mean±S.E.M, an unpaired two-tailed Student t-test: $P^{**}<10^{-2}$) (B) Representative FACS plots of CD206 stained WT and AKAP12KO BMDMs in control gel (orange), WT pCMCs-gel (blue) and AKAP12KO pCMCs-gel (red). CD206-negative controls are shown in black. CD206 fluorescence intensities of BMDMs are normalized to BMDMs in WT pCMCs-gel per group. (n=4 for all group, mean±S.E.M, an unpaired two-tailed Student t-test: $P^{**}<10^{-2,}$ $P^{*}<0.05$).

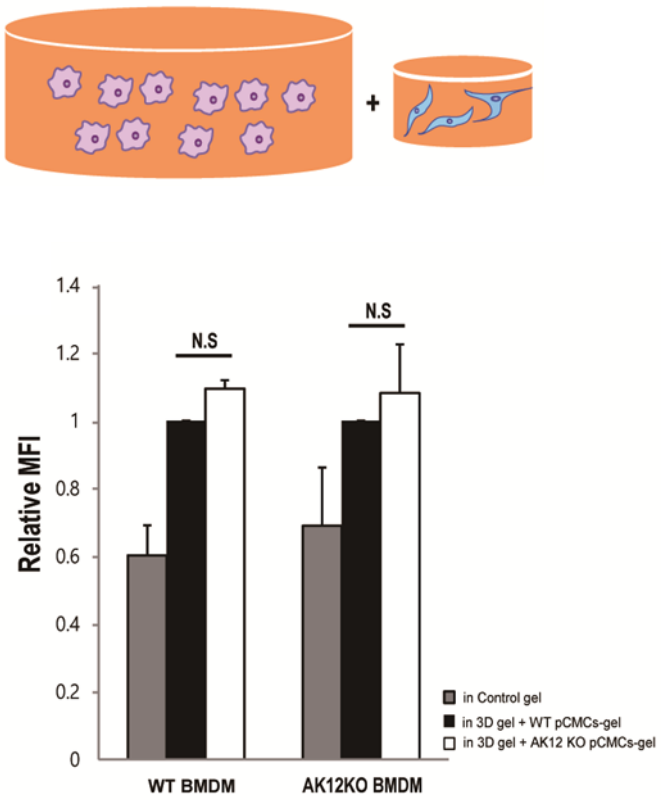

Figure 49. Soluble factors from WT or AKAP12 KO pCMCs don't lead to difference between macrophage polarity of WT and AKAP12 KO BMDMs. WT or AKAP12 KO $5x10^5$ BMDMs were seeded in collagen gels and cultured with none, WT pCMCs-gel and AKAP12 KO pCMCs-gel and then CD206 intensities were measured by FACS (n=3 for all group, mean±S.E.M, an unpaired two-tailed Student t-test: N.S: non-significant)

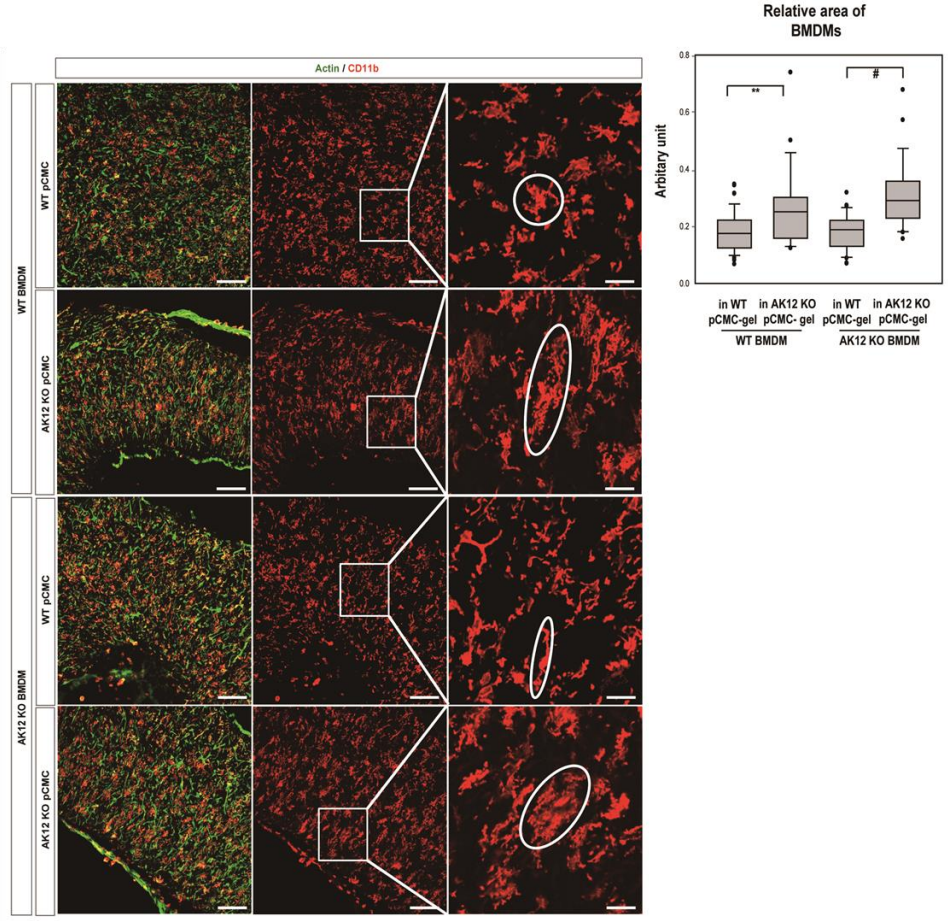
Actin / CD11b
WT BMDM
AK12 KO BMDM
WT pCMC
AK12 KO pCMC
WT pCMC
AK12 KO pCMC
Relative area of BMDMs
Arbitary unit
0.0
0.2
0.4
0.6
0.8
**
#
in WT pCMC-gel
in AK12 KO pCMC- gel
in WT pCMC-gel
in AK12 KO pCMC-gel
WT BMDM
AK12 KO BMDM

Figure 50. AKAP12 KO pCMCs-gel produces larger macrophages than WT pCMCs-gel. Representative confocal imaging of WT or AKAP12 KO MPs in WT or AKAP12 KO pCMCs mediated gels. Representative macrophages are magnified and marked by white circle. Bars: 100 μm (n=2). Box plots of relative area of WT or AKAP12KO MPs in WT or AKAP12KO pCMCs-gels. Middle line in box represents the median, lower box bound the first quartile, upper box bound the third quartile, whiskers the 95% confidence interval of the mean, and circles are outliers from 95% confidence interval. At least 28 macrophages were selected per group. Two independent experiments were performed. Sclae bars: 100 μm (mean±S.E.M, an unpaired two-tailed Student t-test: $P^{\#}<10^{-5,}$ $P^{**}<10^{-2}$)

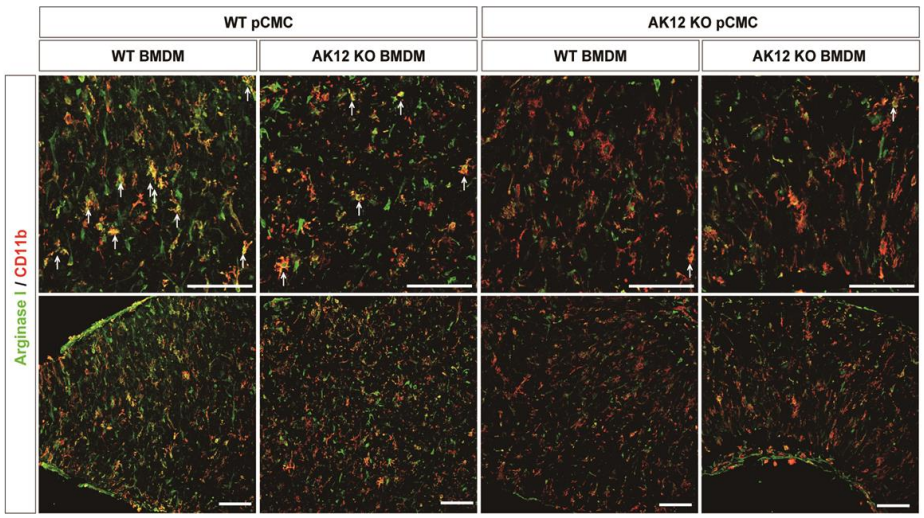

Figure 51. Arginase I+ macrophages are diminished in AKAP12 KO pCMCs-gel. Each Collagen gel sections were immunostained with antibodies against arginase I and CD11b. Sclae bars: 100 μm

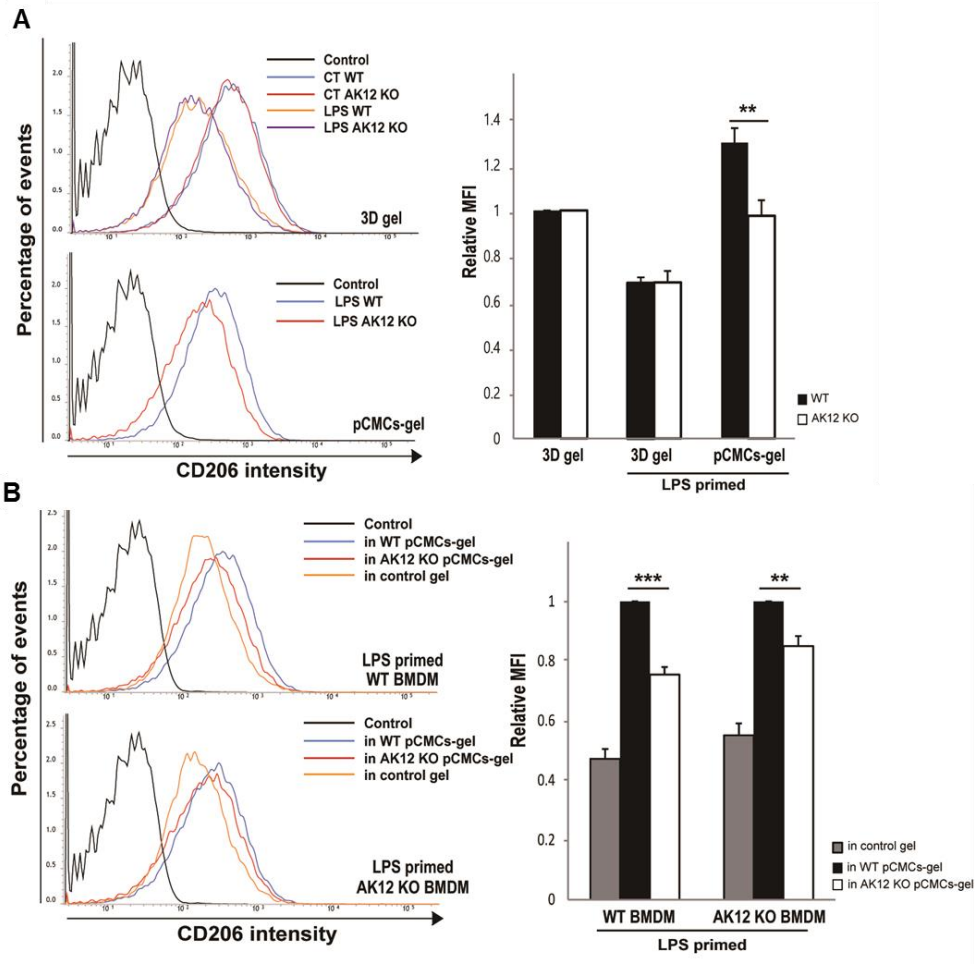
A
Percentage of events
Control
CT WT
CT AK12 KO
LPS WT
LPS AK12 KO
3D gel
Control
LPS WT
LPS AK12 KO
pCMCs-gel
CD206 intensity
Relative MFI
**
WT
AK12 KO
3D gel
3D gel
pCMCs-gel
LPS primed
B
Percentage of events
Control
in WT pCMCs-gel
in AK12 KO pCMCs-gel
in control gel
LPS primed
WT BMDM
Control
in WT pCMCs-gel
in AK12 KO pCMCs-gel
in control gel
LPS primed
AK12 KO BMDM
CD206 intensity
Relative MFI
***
**
in control gel
in WT pCMCs-gel
in AK12 KO pCMCs-gel
WT BMDM
AK12 KO BMDM
LPS primed

Figure 52. LPS primed macrophages are more polarized to M2 macrophages in WT pCMCs-gel than in AKAP12 KO pCMCs-gel. (A) Representative FACS plots of CD206 stained control WT (blue in upper plots) or AKAP12KO (red in upper plots) BMDMs in gel or LPS primed WT (orange in upper plots) or AKAP12KO (purple in upper plots) MPs in gel and LPS primed WT (blue in lower plots) or AKAP12KO (red in lower plots) BMDMs in pCMCs-gel. CD206-negative controls are shown in black. CD206 fluorescence intensity of macrophages are normalized to WT or AKAP12KO control macrophages in gels (n=3 for all group, mean±S.E.M, an unpaired two-tailed Student t-test: P***<10-3, P**<10-2, P*<0.05). (B) Representative FACS plots of CD206 stained LPS primed WT or AKAP12KO BMDMs in control gel (orange), WT pCMC-gel (blue) and AKAP12KO pCMC-gel (red). CD206-negative controls are shown in black. CD206 fluorescence intensity of macrophages are normalized to BMDMs in WT CMC-gels (n=3 for all group, mean±S.E.M, an unpaired two-tailed Student t-test: P***<10-3, P**<10^{-2}, P*<0.05).

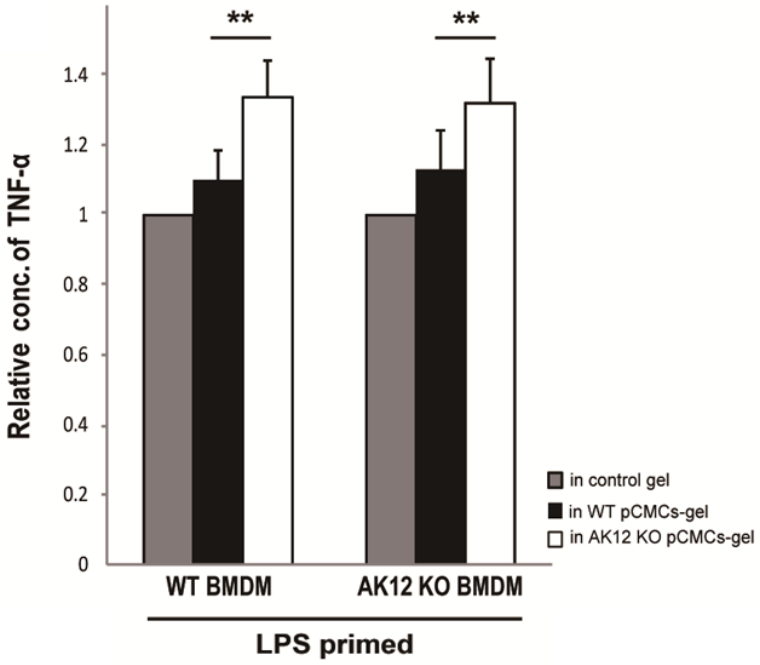

Figure 53. Concentration of TNF-α of BMDMS are higher in AKAP12 KO pCMCs-gel than in WT pCMCs-gel. Relative expression of TNF-α in media of WT or AKAP12KO MP in control gel, WT pCMCs-gel or AKAP12KO pCMCs-gel is assessed by ELISA. (n=3 for all group, mean±S.E.M, an unpaired two-tailed Student t-test: P***<10-3, P**<10^{-2})

8. The expression of AKAP12 regulates focal adhesion in colon mesenchymal cells

To investigate how AKAP12+ CMC promotes tissue contraction during recovery, I investigated the relationship between AKAP12 and focal adhesion maturation which generates strong forces in cells. Indeed, AKAP12 is localized to focal adhesions of WT pCMCs (Figure 54). I also detected that focal adhesions were increased in the WT mucosa than in the AKAP12 KO mucosa (Figure 55). Then, I tried to find the molecules that regulate the AKAP12 expression during intestinal recovery. Raldh2, a retinoic acid (RA) biosynthetic enzyme, was reported to be upregulated in M2 macrophages (Broadhurst et al., 2012). The ramified macrophages in the contracted colon mucosa also expressed more Raldh2 than the round macrophages in less-contracted mucosa (Figure 56). Transforming growth factor-β1 (TGF-β1) was previously reported to be expressed in inflamed colon, have a role in tissue recovery (Del Zotto et al., 2003; Li et al., 2006; Mucida et al., 2009). Notably, the expression of AKAP12 was downregulated by treatment with TGF-β1, and its expression was restored by RA in a dose-dependent manner (Figure

57). Along with the respective decrease and restoration of the AKAP12 expression, the number of focal adhesions was decreased by TGF-β1 and reversed by RA. In contrast, TGF-β1 and RA didn’t affect the number of focal adhesion in AKAP12 KO pCMCs (Figure 58). Together, these data indicate that the AKAP12 expression promotes the formation of focal adhesion in colon mesenchymal cells during intestinal recovery.

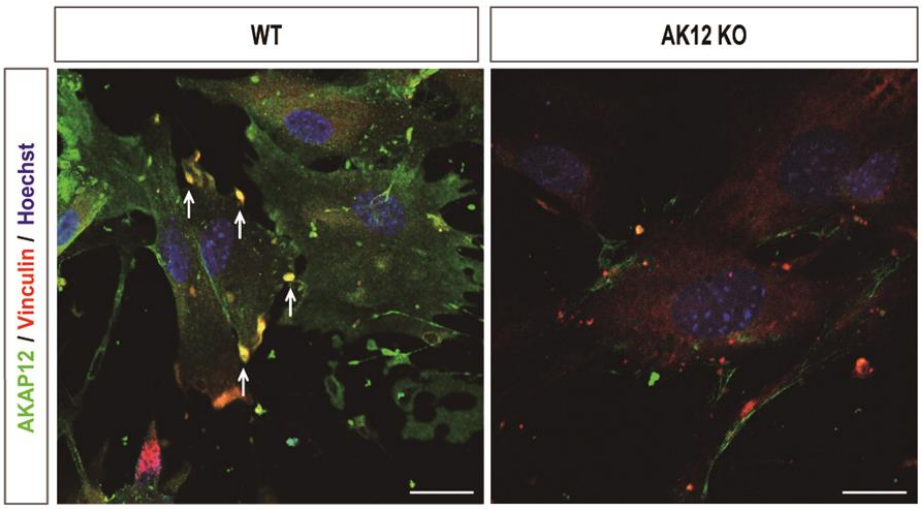

Figure 54. AKAP12 is co-localized to focal adhesion protein. WT and AKAP12 KO primary colon mesenchymal cells were immunostained with antibodies against AKAP12 and vinculn and cell nuclei were counterstained with Hoechst33342. Co-localization are marked by white arrows. Sclae bars: 25 μm

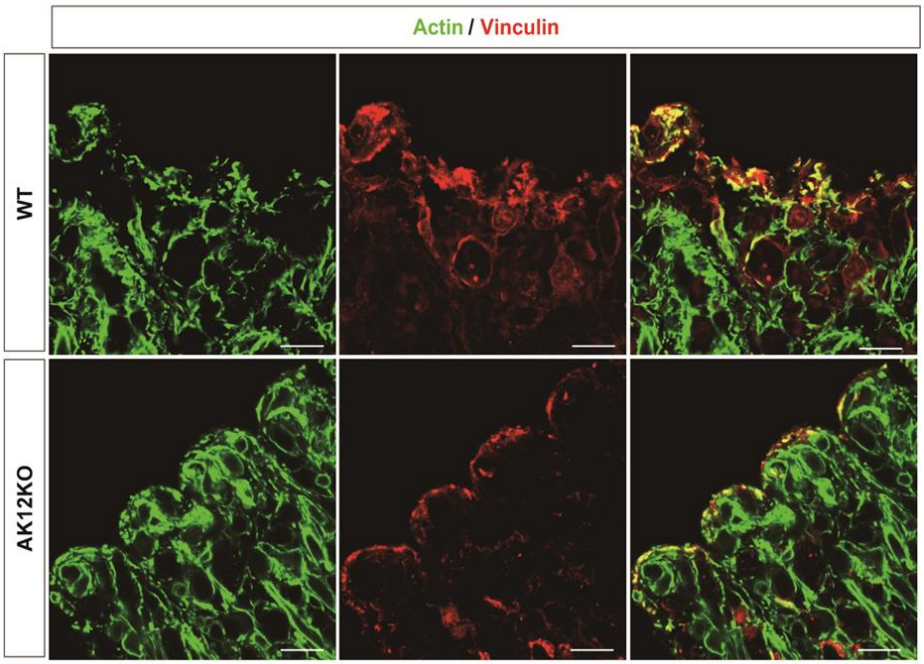

Figure 55. AKAP12 KO inflamed colon mucosa shows smaller and fewer focal adhesions than WT inflamed colon mucosa. Inflamed colon sections of WT and AKAP12 KO mice were immunostained with antibody against vinculin and stained with phalloidin. Sclae bars: 25 μm

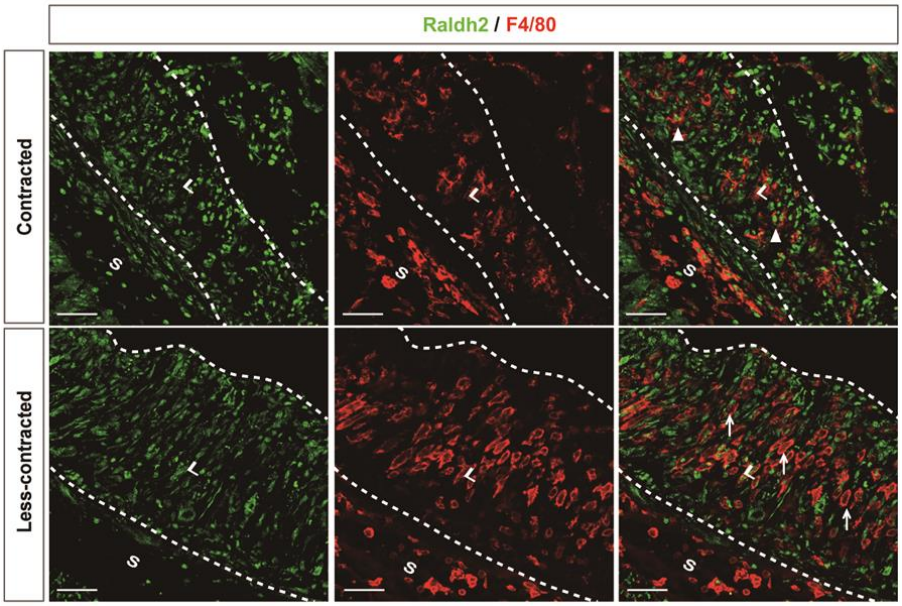

Figure 56. Raldh2 expression is higher in ramifed macrophages in the contracted mucsosa than in round macrophages in the less-contracted mucosa. Inflamed WT colon sections were immunostained with antbodies against Raldh2 and F4/80. Raldh2+ ramified macrophages in contracted part are indicated by arrowheads and Raldh2- round macrophages in less contracted area are indicated by arrows. Sclae bars: 100 μm.

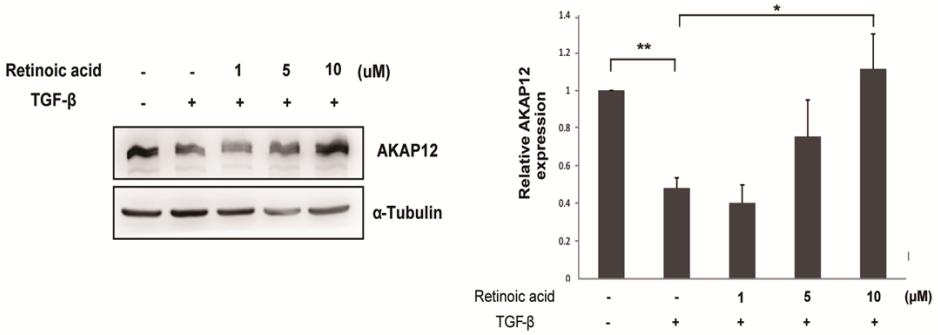

Figure 57. AKAP12 expression is regulated by the TGF-β and Retinoic acid. Representative immunoblots of AKAP12 and α-tubulin in lysate of WT pCMCs when treated with DMSO, TGF-β or TGF-β and RA (1, 5, 10 μM). Densitometries of AKAP12 normalized by α-tubulin in each group are performed by ImageJ program. (n=3 per group, mean± S.E.M, an unpaired and two-tailed t-test: $P^{**}<0.01$, $P^{*}<0.05$)

).

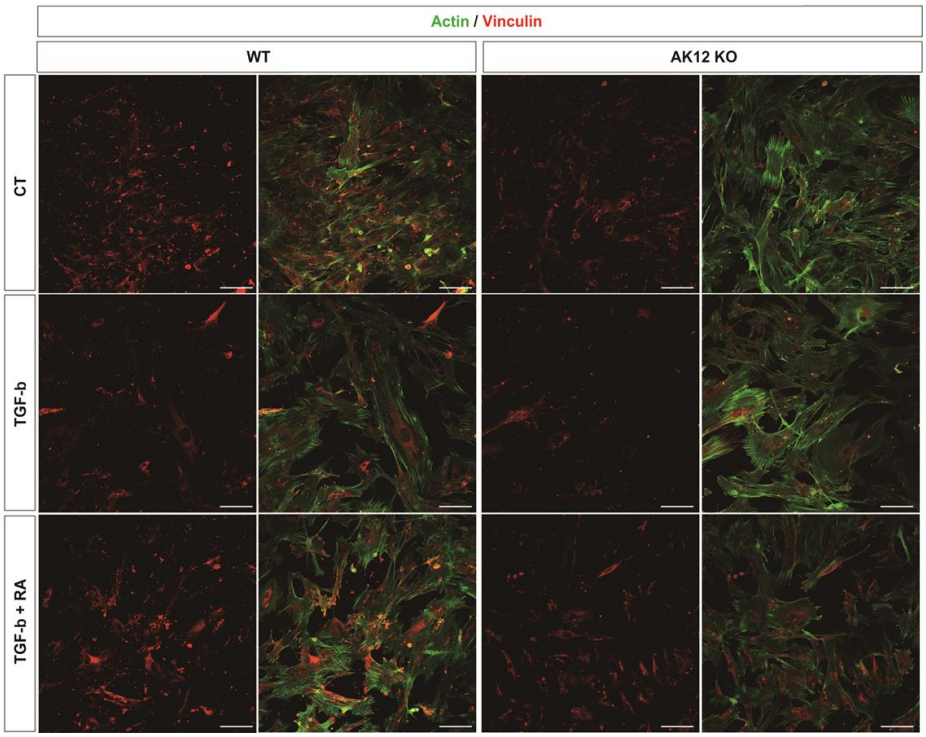

Figure 58. AKAP12 regulates focal adhesion. WT or AKAP12 KO pCMCs were treated with vehicle, TGF-β and RA (10 μM) and then, after 48hr, these cells were immunostained with antibody against vinculin and stained with phalloidin. Scale bars: 100 μm.

9. AKAP12 expression is correlated with the pathways regulating mechanical process and M2 marker in IBD patients and colitis-induced mice

In addition, bioinformatic analysis of the publically available GEO database showed that the gene clusters that were significantly changed during intestinal inflammation of human and mice were involved in focal adhesion, ECM-receptor interaction, and cytoskeletal regulation (Figure 59A and B). Gene clusters highly correlated with the AKAP12 expression in colitis were also involved in the focal adhesion and ECM-receptor interaction (Figure 60). Furthermore, the expression of CD206, an M2 macrophage marker, was positively correlated with the AKAP12 expression in both human and mouse (Figure 61). These bioinformatics data support the notion that the mechanical environment is significantly altered during intestinal inflammation and the AKAP12 expression is linked to M2 macrophage phenotypes in both human and mouse.

A

GSE 38713

Category	Term	Genes	p value
KEGG_PATHWAY	Focal adhesion	87	1.70E-04
KEGG_PATHWAY	Cell adhesion molecules	57	2.80E-03
KEGG_PATHWAY	ECM-receptor interaction	36	2.20E-02

B

GSE 22307

Category	Term	Genes	p value
KEGG_PATHWAY	ECM-receptor interaction	35	4.50E-07
KEGG_PATHWAY	Focal adhesion	64	6.00E-07
KEGG_PATHWAY	Regulation of actin cytoskeleton	66	4.20E-06

Figure 59. Molecular pathway related mechanical processes of the cell are significantly changed in the intestinal inflammation. (A) KEGG pathway shows involvement pathway of differentially expressed genes (DEGs) between non-patients and ulcerative colitis patients (Total genes: 7045, $p < 0.001$). Analysis of DEGs was performed by GEO2R. (B) KEGG pathway shows involvement pathway of differentially expressed gene in DSS 0, 2, 4 and 6 day (Total genes :3899, $p < 0.001$). Analysis of DEGs was performed by GEO2R.

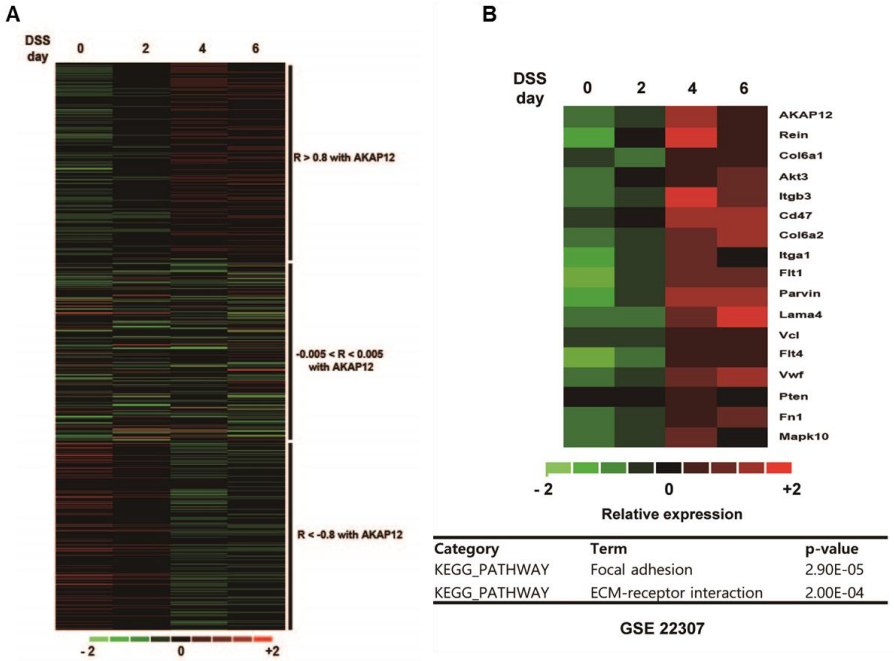

Figure 60. Genes correlated AKAP12 expression are involved in the focal adhesion and ECM-receptor interaction. (A) Heatmap of gene expressions which is positive, none and negative correlated with AKAP12 expression in DSS 0, 2, 4 and 6 day of GEO dataset (GSE22307) **(B)** Heatmap of genes highly correlated with AKAP12 expression and involved in focal adhesion and ECM-receptor interaction in DSS induced colitis mice of GEO dataset (GSE22307). KEGG pathway shows involvement pathway of highly correlated genes with AKAP12 expression (Total genes: 418, r > 0.8 with AKAP12).

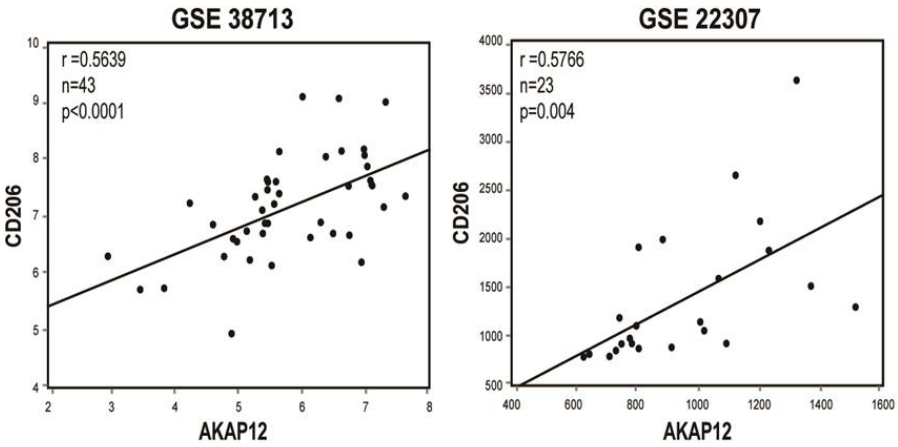

Figure 61. CD206 expression is highly correlated with AKAP12 expression. Scatter plots showing the correlation of AKAP12 expression with CD206 expression in a GEO dataset (GSE38713, GSE22307). The r value was calculated via Spearman's rank correlation coefficient analysis.

DISCUSSON

In this study, I found that AKAP12 function as an ECM regulator during tissue contraction. ECM contraction stimulated by AKAP12+ mesenchymal cells subsequently provides physical cues that promote ramified and non-inflammatory macrophages. In contrast, under AKAP12-deficient condition, the ECM structure has a loose and extended structure, which stimulates the production of round macrophages rather than ramified macrophages (Figure 62). Thus, AKAP12+ mesenchymal cells contribute to ameliorating intestinal inflammation through generating M2 macrophages indirectly during late stage of recovery (Figure 63). In addition, as M2 macrophages also promote tissue remodelling, these macrophages and tissue contraction form the positive feedback loop during recovery. Our findings provide a valuable insight for understanding the role of a dynamically changing physical environment on the functional phenotype of macrophage during recovery.

Much of our current understanding of how the mechanical environment influences macrophage phenotype has come from the field of biomaterials. The shape of macrophages is round on a flat

substrate, but becomes elongated on rough and fibrous substrates (McWhorter et al., 2015). In addition, elongated macrophages show an increase in M2 properties and a reduction in M1 properties (McWhorter et al., 2013). Accordingly, our results indicate that tissue contraction provides rough and fibrous substrate to macrophages, which in turn generates ramified macrophages (Figure 16). These ramified macrophages showed M2 macrophage properties similar to the in vitro results (Figure 24). However, it should be noted that there is a difference in the shapes of ramified and elongated macrophages. I consider that this difference is attributable to the dimension effect. Elongated macrophages in the 2D condition correspond to ramified macrophages in the 3D condition.

Although mechanical differences were observed between the DSS-induced colitis of WT and AKAP12 KO, in vivo conditions trigger many other differences between induced colitis in WT and AKAP12KO, which can influence macrophage polarization. Therefore, I designed experimentally remodelled collagen gels using WT or AKAP12 KO CMCs. Collagen gel contraction mimics matrix reorganization during the tissue-healing phase (Bell et al., 1979). In addition, among CMCs and BMDMs inserted into collagen gels, only

CMCs have the ability to organize collagen gels (Figure 46B), AKAP12 is only expressed in CMCs (Figure 46A), and WT or AKAP12 KO BMDMs did not display a difference in polarity (Figure 48A). However, there is still the possibility that secretion of a soluble factor from different CMCs affects the functional phenotype of macrophages. To overcome this problem, BMDMs and CMCs were cultured in the same well, but in different collagen gels, which can only share soluble factors. The effect of soluble factors from the CMCs of WT or AKAP12 KO mice on macrophage polarization was similar (Figure 48A and 49). Thus, through the in vitro experiments performed under limited experimental conditions, I confirmed our in vivo results that AKAP12+ mesenchymal cells drive M2 macrophage generation through modulating the mechanical environment. In collagen gels, the shape of BMDMs in both the WT CMCs-gel and AKAP12 KO CMCs-gel was ramified, although cell size differed (Figure 50). Although the CD206 expression that is normalized to BMDMs in the WT CMCs-gel is relatively lower in the AKAP12 KO pCMCs-gel than in the WT pCMCs-gel, original CD206 expression of both BMDMs in the WT pCMCs-gel and AKAP12 KO pCMCs-gel was very high (Figure 48A). In the process of gaining primary

macrophages, BMDMs are highly polarized to the M2 phenotype. This is the reason why I assumed that BMDMs inserted in the the WT pCMCs-gel polarize to a deeper M2 side than BMDMs in the AKAP12 KO pCMCs-gel

Further studies need to determine the mechanism under AKAP12+ mesenchymal cells mediated tissue contraction. Mesenchymal cells may need strong forces to contract the matrix as the external environment is converted to a denser matrix during recovery. AKAP12 has been reported to co-localize with focal adhesion and to promote focal adhesion maturation, which generates strong forces in cells (Gardel et al., 2010; Su et al., 2013; Tomasek et al., 2002). Similar with these previous results, I also found that AKAP12 is co-localized with focal adhesion in colon mesenchymal cells (Figure 54) and intend to examine the mechanism whereby AKAP12 regulates focal adhesion maturation in these cells. I recently reported that expression of AKAP12 is regulated by RA and TGF-β1 in CNS injury. These factors function also as upstream regulators of AKAP12 expressin in colon mesenchymal cells (Figure 57). Furthermore, I found that ramified macrophages in contracted colon mucosa also expressed more Raldh2 than round macrophages in less-contracted

mucosa, implying that there are higher RA concentrations in contracted mucosa than in less-contracted mucosa. Thus, during intestinal inflammation recovery, ramified macrophages can promote the upregulation of AKAP12 in colon mesenchymal cells through increasing the RA concentration of surrounding microenvironment, which means positive feedback loop between M2 macrophages and colon mesenchymal cells. RA and TGF-β1 are known to ameliorate several inflammatory diseases including inflammatory bowel dieases (Mucida et al., 2009). There is thus a possibility that RA and TGF-β1 regulate the immune response and inflammation via AKAP12. Therefore, elucidating the connections among AKAP12, RA and TGF-β1 will provide insights for uncovering the mechanism of intestinal inflammation.

In this study, I used a DSS-induced colitis model that resembles the pathogenesis of IBD. IBD is a complex disease that occurs as a result of the interaction of environmental and genetic factors leading to immunological responses and inflammation in the intestine (Baumgart and Carding, 2007). Therefore, IBD may require immunosuppression and a reduction of inflammation for the control of symptoms with anti-inflammatory drugs. Active changes of

mechanical environment occur in IBD patients (Figure 59A) and our results demonstrate that the physical environment contributes to regulating the inflammatory response of intestinal inflammation. Thus, regulation of the physical environment may represent a new therapeutic target for IBD.

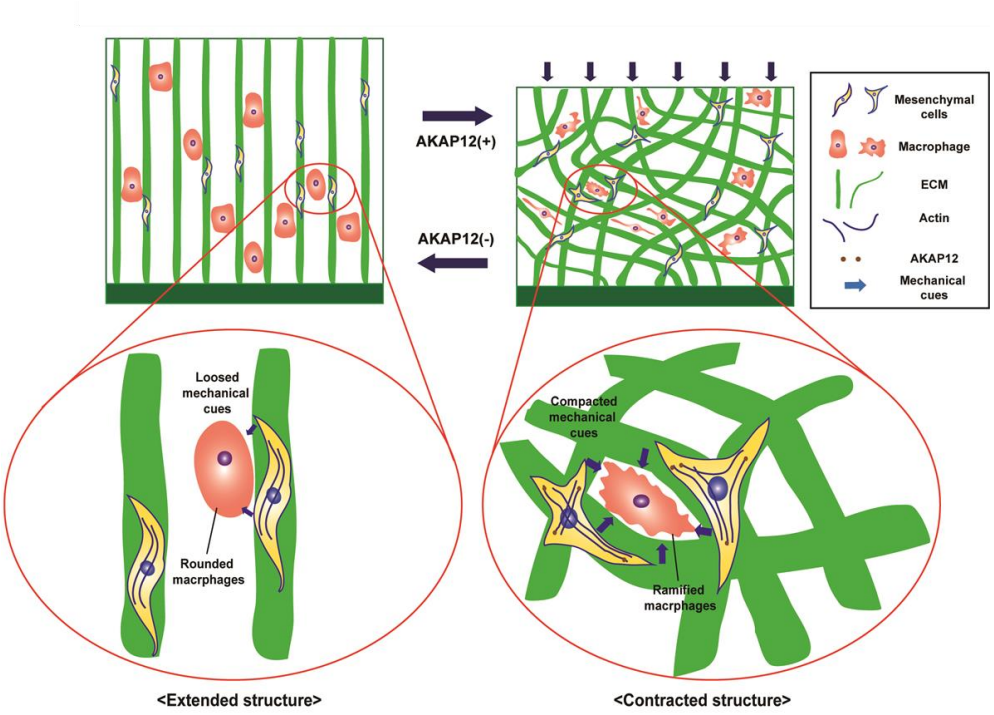

Figure 62. Schematic models depicting effect of AKAP12 on tissue structure that provides macrophages to physical cues AKAP12 induces the tissue contraction that generates contracted mechanical cues. Then, macrophages sensing these cues shift to their shapes as ramified form and polarize their functional phenotype to M2 side.

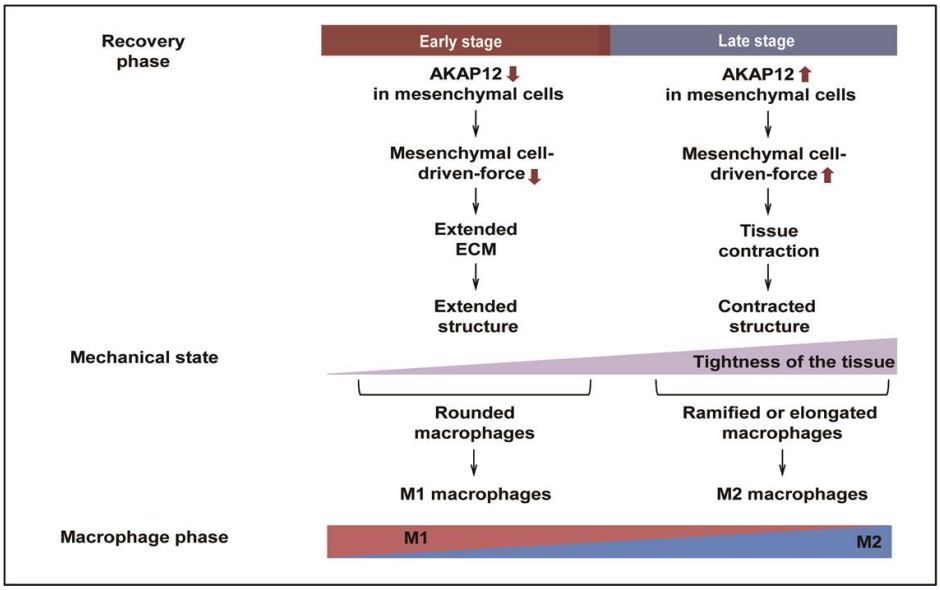

Figure 63. The diagram for the regulation mechanism of mechanical dynamics and macrophage phenotypes during recovery phase In early stage of recovery, AKAP12 expression was downregulated, which promotes extended ECM structures. These loose structures generate round macrophages, skewing to M1 macrophage. On the other hand, in late stage of recovery, the expression of AKAP12 is restored in mesenchymal cells which exert larger forces through larger focal adhesion. These forces generate tissue contraction which contributes to produce ramified M2 macrophage.

Conclusion

1. AKAP12 in colon mesenchymal cells contributes to contraction of colon mucosa during recovery after intestinal inflammation.

2. Tissue contraction generates tight ECM structures that drive ramified M2 macrophages during intestinal recovery.

3. AKAP12 ameliorates the intestinal inflammation via constructing ECM that promotes M2 polarization of macrophages.

4. Restored mechanical environment contributed by M2 macrophages during tissue healing phase provides macrophages to physical cues that leads to M2 polarization, which build positive feedback loop.

5. Collectively, these findings may provide insight for understanding the role of dynamic changing physical environment on functional phenotype of macrophage.

REFERENCES

Ahn, B.J., Le, H., Shin, M.W., Bae, S.J., Lee, E.J., Wee, H.J., Cha, J.H., Lee, H.J., Lee, H.S., Kim, J.H.*, et al.* (2014). Ninjurin1 deficiency attenuates susceptibility of experimental autoimmune encephalomyelitis in mice. J Biol Chem *289*, 3328-3338.

Akakura, S., and Gelman, I.H. (2012). Pivotal Role of AKAP12 in the Regulation of Cellular Adhesion Dynamics: Control of Cytoskeletal Architecture, Cell Migration, and Mitogenic Signaling. J Signal Transduct *2012*, 529179.

Akakura, S., Huang, C., Nelson, P.J., Foster, B., and Gelman, I.H. (2008). Loss of the SSeCKS/Gravin/AKAP12 gene results in prostatic hyperplasia. Cancer Res *68*, 5096-5103.

Baumgart, D.C., and Carding, S.R. (2007). Inflammatory bowel disease: cause and immunobiology. Lancet *369*, 1627-1640.

Bell, E., Ivarsson, B., and Merrill, C. (1979). Production of a tissue -like structure by contraction of collagen lattices by human fibroblasts of different proliferative potential in vitro. Proc Natl Acad Sci U S A *76*, 1274-1278.

Broadhurst, M.J., Leung, J.M., Lim, K.C., Girgis, N.M., Gundra, U.M., Fallon, P.G., Premenko-Lanier, M., McKerrow, J.H., McCune, J.M., and Loke, P. (2012). Upregulation of retinal dehydrogenase 2 in alternatively activated macrophages during retinoid-dependent type-2 immunity to helminth infection in mice. PLoS Pathog *8*, e1002883.

Cao, Q., Harris, D.C., and Wang, Y. (2015). Macro phages in kidney injury, inflammation, and fibrosis. Physiology (Bethesda) *30*, 183-194.

Cha, J.H., Wee, H.J., Seo, J.H., Ahn, B.J., Park, J.H., Yang, J.M., Lee, S.W., Kim, E.H., Lee, O.H., Heo, J.H.*, et al.* (2014a). AKAP12 mediates barrier functions of fibrotic scars during CNS repair. PLoS One *9*, e94695.

Cha, J.H., Wee, H.J., Seo, J.H., Ahn, B.J., Park, J.H., Yang, J.M., Lee, S.W., Lee, O.H., Lee, H.J., Gelman, I.H.*, et al.* (2014b). Prompt meningeal reconstruction mediated by oxygen-sensitive AKAP12 scaffolding protein after central nervous system injury. Nat Commun *5*, 4952.

Chassaing, B., Aitken, J.D., Malleshappa, M., and Vijay-Kumar, M. (2014). Dextran sulfate sodium (DSS) -induced colitis in mice. Curr Protoc Immunol *104*, Unit 15 25.

Chaudhuri, O., Koshy, S.T., Branco da Cunha, C., Shin, J.W., Verbeke, C.S., Allison, K.H., and Mooney, D.J. (2014). Extracellular matrix stiffness and composition jointly regulate the induction of malignant phenotypes in mammary epithelium. Nat Mater *13*, 970-978.

Chinetti-Gbaguidi, G., Baron, M., Bouhlel, M.A., Vanhoutte, J., Copin, C., Sebti, Y., Derudas, B., Mayi, T., Bories, G., Tailleux, A., *et al.* (2011). Human atherosclerotic plaque alternative macrophages display low cholesterol handling but high phagocytosis because of distinct activities of the PPARgamma and LXRalpha pathways. Circ Res *108*, 985-995.

Choi, Y.K., Kim, J.H., Kim, W.J., Lee, H.Y., Park, J.A., Lee, S.W., Yoon, D.K., Kim, H.H., Chung, H., Yu, Y.S., *et al.* (2007). AKAP12 regulates human blood-retinal barrier formation by downregulation of hypoxia-inducible factor-1alpha. J Neurosci *27*, 4472-4481.

Del Zotto, B., Mumolo, G., Pronio, A.M., Montesani, C., Tersigni, R., and Boirivant, M. (2003). TGF -beta1 production in inflammatory bowel disease: differing production patterns in Crohn's disease and ulcerative colitis. Clin Exp Immunol *134*, 120-126.

Folkman, J., and Moscona, A. (1978). Role of Cell -Shape in Growth-Control. Nature *273*, 345-349.

Gabbiani, G., Ryan, G.B., and Majne, G. (1971). Presence of modified fibroblasts in granulation tissue and their possible role in wound contraction. Experientia *27*, 549-550.

Gardel, M.L., Schneider, I.C., Aratyn-Schaus, Y., and Waterman, C.M. (2010). Mechanical integration of actin and adhesion dynamics in c ell migration. Annu Rev Cell Dev Biol *26*, 315-333.

Gelman, I.H. (2010). Emerging Roles for SSeCKS/Gravin/AKAP12 in the Control of Cell Proliferation, Cancer Malignancy, and Barriergenesis. Genes Cancer *1*, 1147-1156.

Hinz, B., and Gabbiani, G. (2003). C ell-matrix and cell-cell contacts of myofibroblasts: role in connective tissue remodeling. Thromb Haemost *90*, 993-1002.

Jetten, N., Roumans, N., Gijbels, M.J., Romano, A., Post, M.J., de Winther, M.P., van der Hulst, R.R., and Xanthoulea, S. (2014). Woun d administration of M2-polarized macrophages does not improve murine cutaneous healing responses. PLoS One *9*, e102994.

Kuhl, A.A., Erben, U., Kredel, L.I., and Siegmund, B. (2015). Diversity of Intestinal Macrophages in Inflammatory Bowel Diseases. Front Immunol *6*, 613.

Kwon, H.B., Choi, Y.K., Lim, J.J., Kwon, S.H., Her, S., Kim, H.J., Lim, K.J., Ahn, J.C., Kim, Y.M., Bae, M.K.*, et al.* (2012). AKAP12 regulates vascular integrity in zebrafish. Exp Mol Med *44*, 225-235.

Li, M.O., Wan, Y.Y., Sanjabi, S., Robertson, A.K., and Flavell, R.A. (2006). Transforming growth factor-beta regulation of immune responses. Annu Rev Immunol *24*, 99-146.

McWhorter, F.Y., Davis, C.T., and Liu, W.F. (2015). Physical and mechanical regulation of macrophage phenotype and function. Cell Mol Life Sci *72*, 1303-1316.

McWhorter, F.Y., Wang, T., Nguyen, P., Chung, T., and Liu, W.F. (2013). Modulation of macrophage phenotype by cell shape. Proc Natl Acad Sci U S A *110*, 17253-17258.

Mosser, D.M., and Edwards, J.P. (2008). Explori ng the full spectrum of macrophage activation. Nat Rev Immunol *8*, 958-969.

Mucida, D., Park, Y., and Cheroutre, H. (2009). From the diet to the nucleus: vitamin A and TGF-beta join efforts at the mucosal interface of the intestine. Semin Immunol *21*, 14-21.

Murray, P.J., Allen, J.E., Biswas, S.K., Fisher, E.A., Gilroy, D.W., Goerdt, S., Gordon, S., Hamilton, J.A., Ivashkiv, L.B., Lawrence, T.*, et al.* (2014). Macrophage activation and polarization: nomenclature and experimental guidelines. Immunity *41*, 14-20.

Murray, P.J., and Wynn, T.A. (2011). Protective and pathogenic functions of macrophage subsets. Nat Rev Immunol *11*, 723-737.

Perse, M., and Cerar, A. (2012). Dextran sodium sulphate colitis mouse model: traps and tricks. J Biomed Biotechnol *2012*, 718617.

Powell, D.W., Pinchuk, I.V., Saada, J.I., Chen, X., and Mifflin, R.C. (2011). Mesenchymal cells of the intestinal lamina propria. Annu Rev Physiol *73*, 213-237.

Rydell-Tormanen, K., Andreasson, K., Hesselstrand, R., Risteli, J., Heinegard, D., Saxne, T., and Westergren-Thorsson, G. (2012). Extracellular matrix alterations and acute inflammation; developing in parallel during early induction of pulmonary fibrosis. Lab Invest *92*, 917-925.

Sica, A., and Mantovani, A. (2012). Macrophage plasticity and polarization: in vivo veritas. J Clin Invest *122*, 787-795.

Stoger, J.L., Gijbels, M.J., van der Velden, S., Manca, M., van der Loos, C.M., Biessen, E.A., Daemen, M.J., Lutgens, E., and de Winther, M.P. (2012). Distribution of macrophage polarization markers in human atherosclerosis. Atherosclerosis *225*, 461-468.

Su, B., Gao, L., Meng, F., Guo, L.W., Rothschild, J., and Gelman, I.H. (2013). Adhesion -mediated cytoskeletal remodeling is controlled by the direct scaffolding of Src from FAK complexes to lipid rafts by SSeCKS/AKAP12. Oncogene *32*, 2016-2026.

Tomasek, J.J., Gabbiani, G., Hinz, B., Chaponnier, C., and Brown, R.A. (2002). Myofibroblasts and mechano -regulation of connective tissue remodelling. Nat Rev Mol Cell Biol *3*, 349-363.

Van Goethem, E., Poincloux, R., Gauffre, F., Maridonneau-Parini, I., and Le Cabec, V. (2010). Matrix architecture dictates three -dimensional migration modes of human macrophages: differential involvement of proteases and podosome-like structures. J Immunol *184*, 1049-1061.

Weischenfeldt, J., and Porse, B. (2008). Bone Marrow -Derived Macrophages (BMM): Isolation and Applications. CSH Protoc *2008*, pdb prot5080.

Wynn, T.A., Chawla, A., and Pollard, J.W. (2013). Macrophage biology in development, homeostasis and disease. Nature *496*, 445-455.

ABSTRACT IN KOREAN (국문 초록)

대장 염증 회복 과정에서 AKAP12 단백질의 기능 연구

대식세포는 염증 후 회복과정에서 그들의 기능적인 표현형을 변환하는 능력인 표현형적인 가소성 (phenotypic plasticity)을 가지고 있다. 이와 동시에 기계적인 환경도 (mechanical environment) 이 과정에서 활발한 변화를 보여준다. 그러나 이러한 기계적인 환경의 역동적인 변화가 어떻게 대식세포의 표현형에 영향을 미치는지는 알려지지 않았다. 본 연구에서는 대장염증 회복과정에서 AKAP12를 발현하는 대장 간엽세포 (colon mesenchymal cell) 에 의해 구성된 세포외 기질 (Extracellular matrix)이 대식세포의 모양을 조절하여 대식세포를 M2 대식세포로 극성화 (polarzation) 시키는 것을 규명하였다.

염증 후 대장에서 선형적이고 느슨한 세포외 기질 구조에서는 원형 형태의 대식세포가 발견되었으며 그 후 회복과정의 수축된 세포외 기질에서는 가지형태의 대식세포가 관찰되었다. 이러한 수축된 구조는 AKAP12 유전자 결손 쥐의 대장 염증 조직 내에서는 관찰되지 않았으며 이를 통해 AKAP12가 대장 염증 조직의 회복과정에서 조직 수축에 관여함을 밝혔다.

흥미롭게도, 원형 형태의 대식세포는 M1쪽으로 극성을 나타냈으며 가지 형태의 대식세포는 주로 M2 표지들을 발현하고 있었다. 결과적으로, 염증 유발 후 회복과정의 AKAP12 유전자 결손 쥐의 대장

에서는 수축된 구조가 잘 형성되지 않았기 때문에 원형 형태의 대식세포가 주로 발견되었으며 M2 표현형을 가진 대식세포의 숫자가 WT 쥐보다 감소되어 있었다. 게다가, AKAP12 유전자 결손 쥐에서 임상적인 증상과 조직의 손상 정도 역시 WT보다 더 심각한 것을 관찰할 수 있었다.

이러한 In vivo실험에서의 결과를 보다 제한된 조건에서 증명하기 위하여, 실험적으로 대장 간엽세포를 통하여 콜라겐 젤 (collagen gel)을 재구성하는 모델을 설계하였다. WT 유래의 대장 간엽세포는 AKAP12 결손 쥐의 대장 간엽세포보다 더 조밀한 콜라겐 젤을 형성하였으며, 이러한 조밀한 구조가 대식세포를 더 M2 형질로 유도하는 것을 관찰하였다.

이러한 결과를 통하여 대장 염증 후 회복에서, 조직의 수축이 대식세포들에게 물리적인 신호를 전달하여 이 세포들을 M2 방향으로 극성화 시키는 것을 규명하였다. 또한, 물리적인 환경을 조절하여 염증을 조절하는 연구를 통하여 대장염증의 새로운 치료 표적 (therapeutic target)이 개발될 것이라 기대된다.

……

주요어 : 주요어 : 대장염증 후 회복, AKAP12, 조직 수축, 조밀한 구조, 대식세포의 형태, M2 대식세포

학 번 : 2011 − 21736